Tropical Cyclone Induced Extreme Wind, Rainfall, and Floods in the Mekong River Basin

Aifang Chen

UNIVERSITY OF GOTHENBURG
Faculty of Science

Doctoral Thesis
University of Gothenburg
Department of Earth Sciences
Gothenburg, Sweden 2020

Supervisor

Professor Deliang Chen, Department of Earth Sciences, Faculty of Science, University of Gothenburg

Co-Supervisor

Professor Roland Barthel, Department of Earth Sciences, Faculty of Science, University of Gothenburg

Examiner

Professor Hans Linderholm, Department of Earth Sciences, Faculty of Science, University of Gothenburg

Cover illustration: Xinyi You and Aifang Chen

Tropical Cyclone Induced Extreme Wind, Rainfall, and Floods in the Mekong River Basin

ISBN 978-91-7833-860-3 (PRINT)
ISBN 978-91-7833-861-0 (PDF)
Internet-ID: http://hdl.handle.net/2077/64068

Printed by Stema Specialtryck AB
Gothenburg, Sweden 2020

SVANENMÄRKET
Trycksak
3041 0234

“If I have seen further, it is by standing on the shoulders of giants”

Isaac Newton (1643 – 1727)

Abstract

Increasing magnitude and frequency of climate extremes under global warming are threatening the socioeconomic development in many parts of the world. The Mekong River Basin (MRB) is a good example for how climate extremes can affect society, as the transboundary MRB has experienced hydroclimate changes and fast socioeconomic development during the past decades. The MRB is a flood-prone area with high flood induced mortality, where heavy monsoon rainfall and tropical cyclones (TCs) landfall are the two main determinants of floods. This thesis focuses on the change in TCs and their associated impacts of extreme wind, rainfall, and floods on the MRB. Findings from this thesis provide an improved understanding of TCs and their impacts, which is useful to mitigate potential consequences of global warming in the MRB and other areas facing similar challenges.

Employing reliable precipitation data, this thesis finds that TC induced rainfall plays a minor role in the annual mean precipitation in the MRB. But TCs are crucial to the occurrence of extreme rainfall events, particularly at the eastern lower basin. TC induced floods amount to about 24.6% of all flood occurrence in the lower riparian countries. TC induced floods cause higher impacts on human mortality and displacement rates than the average of floods induced by all possible causes do. Moreover, future projection shows increases in the future TC intensity under the Representative Concentration Pathway (RCP) 8.5 scenario.

Overall, this thesis reveals that climate extremes, such as TC associated rainfall and floods, can substantially affect society, in terms of the high TC induced extreme rainfall and great human mortality and displacement rates caused by TC induced floods. The projected future intensified TCs indicate increasing TC risks.

Keywords: Mekong River Basin, Climate extremes, Tropical cyclones, Precipitation, Floods, Satellite data, Reanalysis data

List of Publications

This thesis consists of a summary (Part I) which is based on the following studies (Part II), referred to in the text by their Roman numerals. The published studies are reprinted with permission from the respective journals:

I. **Chen A.**, D. Chen, C. Azorin-Molina, 2018: Assessing reliability of precipitation data over the Mekong River Basin: A comparison of ground-based, satellite, and reanalysis datasets. *International Journal of Climatology*, DOI: 10.1002/joc.5670

II. **Chen A.**, C. H. Ho, D. Chen, C. Azorin-Molina, 2019: Tropical cyclone rainfall in the Mekong River Basin for 1983-2016. *Atmospheric Research*, DOI: 10.1016/j.atmosres.2019.04.012

III. **Chen A.**, M. Giese, D. Chen, 2020: Flood impact on Mainland Southeast Asia between 1985 and 2018 -- The role of tropical cyclones. *Journal of Flood Risk Management*. DOI: 10.1111/jfr3.12598

IV. **Chen A.**, K. Emanuel, D. Chen, C. Lin, F. Zhang, 2020: Rising future tropical cyclone-induced extreme winds in the Mekong River Basin. *Science Bulletin*, DOI: 10.1016/j.scib.2019.11.022

Contributions: The co-authorship of the articles reflects the collaborative nature of the underlying researches. Regarding paper I, II, III, and IV, A. Chen was responsible for study design and data analysis, and has led the writing.

Selected publications not included in the thesis:

I. **Chen A.**, A. Chen, O. Varis, D. Chen, 2020: Continuous forest loss in the Tonle Sap Lake area in the 21st Century. Under review

II. Sun L., Y. Cai, **A. Chen**, D. Zamora, F. Jaramillo, 2020: Zooming-in to the hydroclimatic effect of impounded reservoirs by nested catchment analysis. Under review

III. Li, R., L. Xu, O. N. Bjørnstad, K. Liu, T. Song, **A. Chen**, B. Xu, Q. Liu, N. C. Stenseth, 2019: Climate-driven variation in mosquito density predicts the spatiotemporal dynamics

of dengue. *Proceedings of the National Academy of Sciences*, DOI: 10.1073/pnas.1806094116

IV. He B., **A. Chen**, W. Jiang, Z. Chen, 2017: The response of vegetation growth to shifts in trend of temperature in China. *Journal of Geographical Sciences*, DOI: 10.1007/s11442-017-1407-3

V. Huang L., B. He, **A. Chen**, H. Wang, J. Liu, A. Lv, Z. Chen, 2016: Drought dominates the interannual variability in global terrestrial net primary production by controlling semi-arid ecosystems. *Scientific Reports*, DOI: 10.1038/srep24639

Acknowledgement

The past four years have been neither easy nor relaxing, but it has been one of the most precious experiences of my life. I would like take this opportunity to express my great appreciation to those who have helped me.

First and foremost, I would like to express my sincere gratitude to my supervisors and my examiner. Prof. Deliang Chen, thank you for offering me this opportunity to study in a harmonious and active academic group. You taught me to think outside the box. I appreciate your patience in listening to me. Your insights have guided me, and your encouragements have stimulated me. You are the most knowledgeable, diligent and respectful man I have ever met. Prof. Roland Barthel and Prof. Hans Linderholm, thank you for being there for me to clear up those messy problems I had.

I would like to thank all my collaborators for the countless hours of fruitful discussion. Your expertise was valuable to my research. The collaboration with you have increased the depth and breadth of my research. Thank you all for the precious opportunities for me to work with you.

Many thanks to my dear colleagues at the Department of Earth Sciences. When I talked about my issues, you listened and gave me insightful advice. The fun time we had during lunch and afterwork made my journey joyful and meaningful.

My dear friends from home and abroad, thank you for your unfaltering friendship. You cheered me up when I was down, you made me braver when I was timid.

Thanks to you all, this PhD journey was worth taking and I look forward to discovering more worthwhile journeys henceforth.

Table of Contents

Summary in English

Extreme weather and climate events (climate extremes), for example tropical cyclones (TCs), are natural hazards that can have extensive impacts on humans and ecosystems. As a consequence of global warming, hydroclimate variability is predicted to be amplified, resulting in higher frequency of climate extremes. Better understanding of climate extremes in the Mekong River Basin (MRB) is vital to human mitigation and adaptation because of the basin's complex interactions among climate, hydrology, and socioeconomic. The hydrological regime in the MRB is dominated by heavy monsoon rainfall and frequent landfalling TCs, leading to seasonal floods. Floods occurring in the basin often cause fatalities and damages. Focusing on the TCs and associated extreme wind, rainfall, and floods in the MRB, this thesis aims to i) advance understanding of changes in TCs and their associated rainfall and floods in the past decades, and ii) project the future change in TC intensity.

The thesis first evaluates the reliabilities of five available gridded precipitation datasets (paper I). Employing the precipitation data with the best performance (the Precipitation Estimation from Remotely Sensed Information using Artificial Neural Networks – Climate Data Record [PERSIANN-CDR]), this thesis finds that TCs only contributed to 2.5% of the annual mean total precipitation in the basin for 1983 – 2016. However, TCs are crucial to the occurrence of extreme precipitation which are able to trigger severe flooding along their moving tracks (paper II). TC induced floods amounted to 24.6% of the flood occurrence in the lower basin's riparian countries (1985 – 2018). Generally, these TC induced floods have caused relatively higher mortality and displacement rates than the average of floods induced by all possible reasons do (paper III). In addition, a dynamical downscaling technique is applied to estimate the future TC change, under the Representative Concentration Pathway (RCP) 8.5 scenario (paper IV). Results show that the return periods of TCs' maximum wind speed influencing the basin would be shorter for 2081 – 2100 compared with 1981 – 2000, indicating increasing intensities of future TCs in the MRB.

The findings present in this thesis reveal the changes in and impacts of TC associated extreme wind, rainfall, and floods on the MRB during the 1980s – 2010s and the potential impact it could have for 2081 – 2100. Conclusively, TCs play a decisive role in carrying extreme precipitation and inducing floods, which claimed disproportionate impacts on the

MRB; and intensified future TCs are projected under high emission scenario. The high mortality rates from floods indicate the vulnerability of local inhabitants to the TCs. Findings from this thesis offer scientific support for a better preparedness and policy making, helping us to achieve a more resilient society.

Sammanfattning på Svenska

Extremt väder och klimathändelser (klimatextrema), till exempel tropiska cykloner (TCs), är naturkatastrofer vilket kan innebära stora faror för oss människor och ekosystem. Som en följd av den globala uppvärmningen förutsägs hydroklimatisk variation att öka, vilket resulterar i högre frekvens av klimatextrema. Bättre förståelse av klimatextrema i Mekong River Basin (MRB) är avgörande för mänsklig beredskap och anpassning på grund av avrinningsområdets komplexa interaktion mellan klimat, hydrologi och socioekonomi. Den hydrologiska regimen i MRB domineras av kraftigt monsunregn och ofta landande TCs, vilket leder till säsongsöversvämningar. Översvämningar som uppstår i avrinningsområdet orsakar ofta levnadsförluster och egendomsskador. Med fokus på TCs och tillhörande extrema vindar, nederbörd och översvämningar syftar denna avhandling att i) främja förståelse för förändringar av TCs och deras tillhörande nederbörd och översvämningar under de senaste decennierna, och ii) projicera den framtida förändringen av TC-intensitet.

Denna avhandling utvärderar först tillförlitligheten av fem tillgängliga nederbördsdata (papper I). Med hjälp av en tillförlitlig nederbördsdata (the Precipitation Estimation from Remotely Sensed Information using Artificial Neural Networks – Climate Data Record [PERSIANN-CDR]), finner denna avhandling att TCs endast bidrog med 2,5% av den årlig genomsnittlig total nederbörden i avrinningsområdet mellan 1983 och 2016. TCs är emellertid avgörande för förekomsten av extremt regn som kan utlösa allvarlig översvämning längs dess rörliga spår (papper II). TC-inducerade översvämningar uppgick till 24,6% av översvämningar i de nedre riparianländerna av floden (1985 – 2018). I allmänhet har dessa TC-inducerade översvämningar orsakat relativt högre dödlighet och förflyttning än medelsnittet av översvämningar orsakade av alla möjliga skäl (papper III). Dessutom en dynamisk nedskalningsteknik används för att uppskatta den framtida TC-förändringen under Representative Concentration Pathway (RCP) 8.5-scenariot (papper IV). Resultaten visar att returperioder av TCs maximal vindhastighet som påverkar avrinningsområdet skulle bli kortare under 2081 – 2100 jämfört med 1981 – 2000, vilket indikerar ökad intensitet av framtida TCs i MRB.

Resultaten som presenteras i denna avhandling avslöjar de förändringar och den påverkan TC-tillhörande extrema vindar, nederbörd och översvämningar hade på MRB under 1980- till 2010-

talet, och potentiellt skulle kunna ha 2081 - 2100. Sammanfattningsvis spelar TCs en avgörande roll att orsaka extremt regn och inducera översvämningar som hävdade en oproportionerlig inverkan på MRB; och intensifierade framtida TCs projiceras under högutsläppsscenariot. Den höga dödligheten från översvämningar indikerar de lokala invånarnas sårbarhet för TCs. Resultaten från denna avhandling erbjuder ett vetenskapligt stöd för bättre beredskap och beslutsfattande, med målet att uppnå ett mer motståndskraftigt samhälle inom MRB och områden med liknande utmaningar.

Popular Science Summary

Extreme weather and climate events (climate extremes), for example tropical cyclones (TCs), are one of the major natural hazards threatening humans and ecosystems. More climate extremes are predicted to occur under future global warming. Advancing the understanding of expected impacts of climate extremes is necessary, and it will be helpful for a better adaptation of society against the rising climate risks. Climate extremes and their impacts in the Mekong River Basin (MRB) in Southeast Asia need to be studied, because the MRB has often been hit by TCs and suffered damages and losses. This thesis aims to better understand i) how TCs change between the 1980s and 2010s; ii) what the impacts are of TC associated rainfall and floods in the MRB; and iii) how TC intensity will change in the future.

This thesis finds that TCs play an important role in extreme rainfall and that TC induced heavy rainfall events often lead to floods. In the basin's riparian countries, about 24.6% of the floods are caused by TCs in 1985 – 2018. Moreover, TC induced floods have resulted in relatively higher impacts on human mortality and displacement rates than the average of all the occurred floods. Future TC intensity is projected to increase in the MRB. This will raise the future TC related risk not only on a local scale, but also on a regional and beyond.

Overall, findings from this thesis show the changes in the past TCs and the high impacts on humans they have by causing heavy rainfall and floods. The projected future of rising TC intensity raises an alarm for the urgency of taking measures to mitigate potential impact of TCs on society.

Abbreviations

Abbreviation	Unit	Description
m a.s.l.	m	meters above sea level
ALLFloods	event	Floods induced by all possible causes
APHRODITE	-	Asian Precipitation – Highly- Resolved Observational Data Integration Towards Evaluation of Water Resources
CFSR	-	Climate Forecast System Reanalysis
CMIP5	-	Coupled Model Intercomparison Project Phase 5
ENSO	-	El Niño-Southern Oscillation
ERA-Interim	-	European Centre for Medium-Range Weather Forecasts interim reanalysis
FLOPROS	-	FLOodPROtection Standards
GCMs	-	Global climate models
GFDL5	-	GFDL-CM3
GPCv1	-	Global Population Count Grid Time Series Estimates, v1
GPWv4	-	Gridded Population of the World, Version 4
HadGEM5	-	HadGEM2-ES
IBTrACS	-	International Best Track Archive for Climate Stewardship
IPSL5	-	IPSLCM5A- LR
MERRA2	-	Modern-Era Retrospective analysis for Research and Applications Version 2
MIROC5	-	MIROC5
MPI5	-	MPI-ESM-MR
MRB	-	Mekong River Basin
MSEA	-	Mainland Southeast Asia
MWS	knot	maximum wind speed
NASA	-	National Aeronautics and Space Administration
NOAA	-	National Oceanic and Atmospheric Administration
NRMSE	-	Normalized root mean-square error
NS	-	Nash–Sutcliffe coefficient of efficiency
PDO	-	Pacific Decadal Oscillation
PERSIANN-CDR	-	Precipitation Estimation from Remotely Sensed Information using

		Artificial Neural Networks – Climate Data Record
r	-	Pearson's correlation coefficient
R20mm	days	Days of heavy precipitation rate ≥ 20 mm day^{-1}
R50mm	days	Days of extremely heavy precipitation rate ≥ 50 mm day^{-1}
RBS	%	Relative bias
RCP	-	Representative Concentration Pathway
SEDAC	-	Socioeconomic Data and Applications Center
SSPs	-	Shared Socioeconomic Pathways
TCFloods	-	Floods induced by tropical cyclones
TCR	mm	Tropical cyclone associated rainfall
TCRC	%	Contribution of TCR to total precipitation
TCs	-	Tropical cyclones
TRMM 3B42	-	Tropical Rainfall Measuring Mission post-real-time research products, version 7, 3B42v7
USD	$	United State Dollars

Part I

– Synthesis –

1 Introduction

Extreme weather and climate events (climate extremes) like droughts, heavy rainfall, floods, and tropical cyclones (TCs) are natural hazards that can have substantial impacts on humans (IPCC 2012). Better understanding the changes of climate extremes and their impacts are essential for human mitigation and adaptation in a changing climate. According to the Clausius-Clapeyron relation, the atmospheric water holding capacity will increase by 7% per degree of warming, resulting in amplified hydroclimate variabilities under global warming (thermodynamics response to climate warming) (Bengtsson 2010; IPCC 2013; Payne et al. 2020). Regional hydroclimate is strongly coupled to changes in the large-scale atmospheric circulations (e.g., El Niño–Southern Oscillation [ENSO]), which are triggered by global warming (dynamics response to climate warming) (Ha et al. 2020; Räsänen et al. 2016; Ward et al. 2014; Payne et al. 2020). The responses of regional hydroclimate in Asian monsoon regions to climate warming have caused increasingly frequent climate extremes, resulting in, for example, floods and droughts (IPCC 2013; Pfahl et al. 2017; Seneviratne et al. 2006) (Figure 1).

Climate extremes can cause human live losses, health problems, and economic damages (Martin 2015; Rappaport 2000, 2014; Zhang et al. 2017b). In Asia, floods, storms/TCs, droughts, heat waves, wildfires, and mass movements, are major disasters linked to climate extremes (CRED 2019). Storms/TCs and floods attributed to 35% and 45% of the total 2681 reported disasters in 1970 – 2012 (WMO 2014). Among the climate extreme disasters, TCs have the most impact on live losses, whereas floods cause greatest property damages (MRC 2015; WMO 2014). Located in Mainland Southeast Asia (MSEA), the Mekong River Basin (MRB) is also heavily affected by TCs and floods, suffering from high human mortality and property damages (MRC 2010a). Taking the MRB as a case study, investigation of climate extreme impacts on environment and socioeconomics advances the understanding of potential consequences of global warming on the society in the MRB and other regions which are similarly affected by TCs and floods.

The MRB has a complex hydroclimate, dominated by the Southwest Asian monsoon- and East Asian monsoon systems (Indian Summer Monsoon, East Asian Monsoon and Western North Pacific Monsoon) (Delgado et al. 2010; Holmes et al. 2009; Räsänen and Kummu 2013; Wang and Ho 2002) and TCs (Darby et al. 2013; MRC 2010a) (Figure 2). Hydroclimate in the MRB is associated with large-scale atmospheric

circulations, e.g., ENSO and Pacific decadal oscillation (PDO) (Delgado et al. 2012; Räsänen and Kummu 2013). For example, the basin is wetter during La Niña years, whereas it's dryer during El Niño years (Delgado et al. 2010). TC activity influencing the basin is also correlated with these large-scale atmospheric circulations (Elsner and Liu 2003; Lee et al. 2012; Walsh et al. 2016). In addition, weakening trends in Indian Summer Monsoon and East Asian Monsoon (monsoon systems influencing the MRB) have been observed (Liu et al. 2019; Swapna et al. 2017). Altogether, global warming and dynamic changes of large-scale circulations potentially induce hydroclimate change and thus affect climate extremes in the MRB (Räsänen and Kummu 2013; Payne et al. 2020).

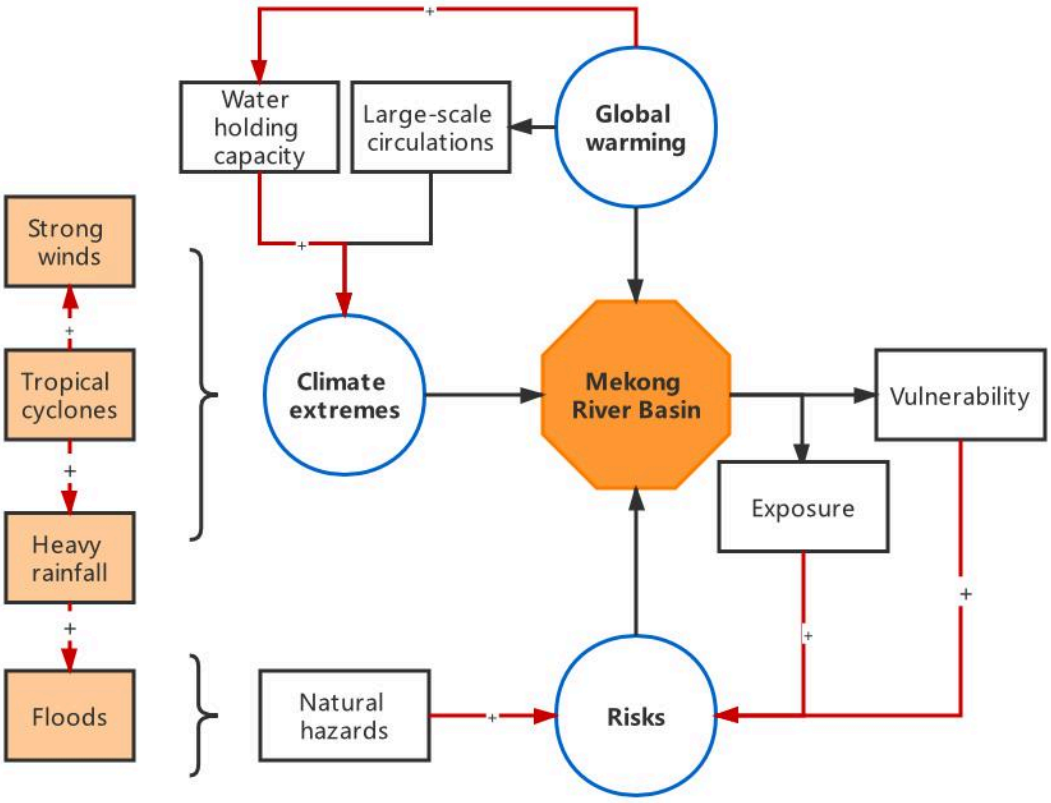

Figure 1. Schematic diagram of tropical cyclones and their impacts on the Mekong River Basin. Global warming, climate extremes and risks are major aspects of the climate change impacts on the Mekong River Basin. Under global warming, the changes and impacts of climate extremes, such as tropical cyclones associated strong wind, heavy rainfall, and floods are main focuses of the thesis. Red lines represent positive feedbacks.

TCs in the MRB are the primary concerns of disaster risk affecting the local inhabitants. Many well-known severe TCs and their associated floods have hit the region that resulted in loss of life and damages to

property. For instance, TC Ketsana in 2009 caused a total of 1.011 billion United State Dollars (USD) in economic losses (MRC 2010b). However, the risk a climate extreme poses on society depends not only on the occurrence of climate extremes themselves, but also the "exposure" and "vulnerability" a society has as a combination of the prevailing environmental and socioeconomic factors (such as population density and underlining assets) (IPCC 2012). Rapid population growth (MRC 2010a; Pech and Sunada 2008) increases the "exposure" in the MRB. Among the riparian countries, Cambodia, Myanmar, and Laos, are of extreme poverty (ASEAN 2017). Particularly in the lower MRB, millions of people depend on the Mekong River for livelihood, but live in poor conditions today (MRC 2010a). These unstable socioeconomic conditions of the basin determine the "vulnerability" of the local inhabitants confronting climate extremes (MRC 2015). Additionally, in the coming decades, the basin population will likely grow and the MRB will experience increases in temperature, precipitation, and floods (Hoang et al. 2016; MRC 2010a; Winsemius et al. 2016). Overall, advanced understandings of changes in TCs and the impacts on the MRB are thus essential in order to be better prepared for the increasing TC associated risk as a result of future climate warming.

On average, there are 6 TCs per year influencing the MRB (1983 – 2016). Given the frequent landfalling TCs and their far-reaching societal impacts, research is needed to promote the understanding of changes in TCs and the associated impacts on the MRB. For example, how do TCs and the associated rainfall (TCR) influence the MRB? To what extent do TC induced floods affect the basin? What is the future change in TC associated extreme wind? This thesis addresses these issues by focusing on TCs and their associated extreme wind, rainfall, and floods. The outcome of this thesis provides scientific evidence of the change in TCs and the impacts on the MRB. With this thesis, we hope to show how regional climate studies can advance our understanding of TC impacts on humans and ecosystems.

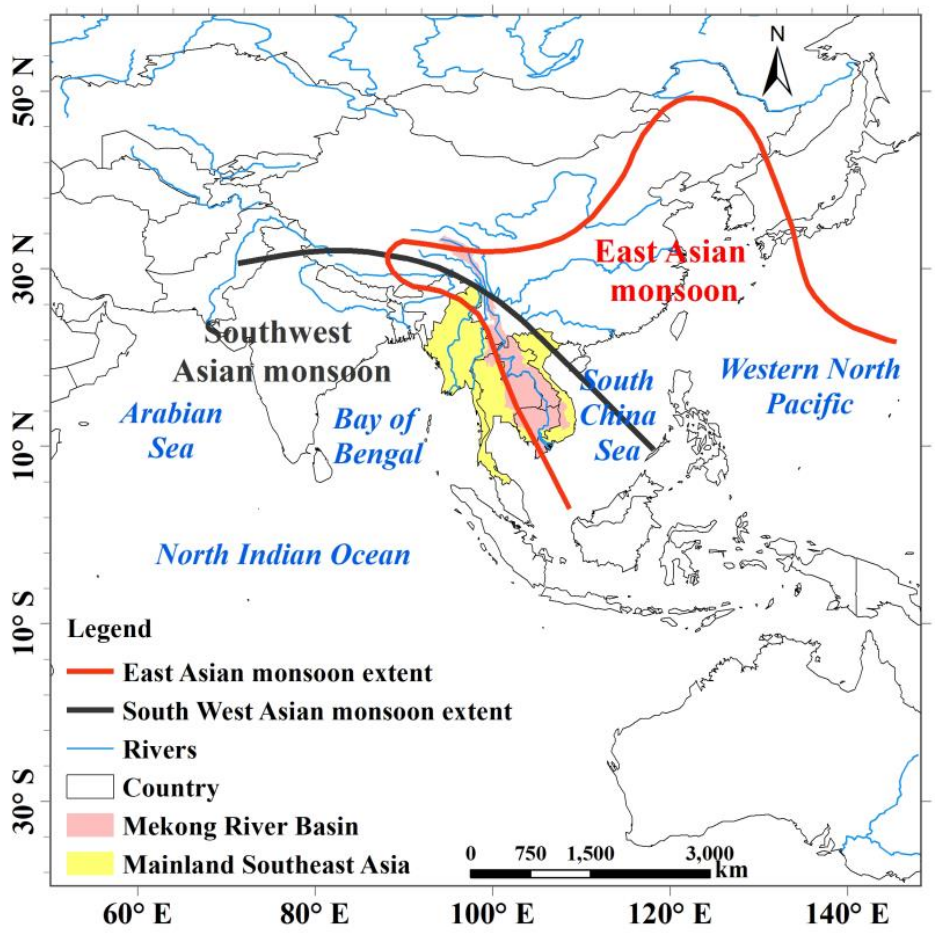

Figure 2. Overview map of the Mainland Southeast Asia and Mekong River Basin. The approximate East Asian monsoon and Southwest Asian monsoon extents were taken from Holmes et al. (2009) and Wang and Ho (2002).

2 Background

2.1 Study Area

The Mekong River is a transboundary river listed as the 10th of the world's longest rivers (MRC 2010a) (Figure 3). It originates from the southeastern Tibetan Plateau at an altitude of 5160 meters above sea level (m a.s.l.) in China, and plunges into the 'Three River Area' characterized by deep gorges and high ridges. The Mekong then flows to the Lancang Basin. These regions make up the upper MRB (MRC 2010a). The four regions in the lower MRB it runs through are Northern Highland, Khorat Plateau, Tonle Sap Basin, and Mekong Delta. After flowing for 4,909 km, the Mekong discharges into the South China Sea in Mekong Delta (MRC 2005, 2010a). In total, the MRB has a spatial coverage of 795,000 km^2 consisting of parts of six countries – China, Myanmar, Laos, Thailand, Cambodia, and Vietnam (MRC 2010a).

Owing to the importance of the Mekong River to the socioeconomic development of the basin, the Mekong River Commission (MRC, http://www.mrcmekong.org/) has been established since the 1995, to coordinate the lower MRB countries' sustainability management of the basin's water resources (Keskinen 2008). A "State of the basin report" was published by the MRC in 2010 to support the basin's development presented in MRC (2010a). According to the report, the hydroclimatic regimes of the Mekong River are mainly controlled by monsoonal climate, with distinct seasonal regimes. The MRB is featured with distinct wet season (June – October) and dry season (November – the following May). The basin is dominated by the Southwest Asian monsoon and East Asian Summer monsoon during the wet season, which transport warm and moist air primarily from Indian Ocean into the basin, contributing to about 70% of the annual precipitation. The Northeast Asian monsoon with its cold, high-pressure system occupies the basin in the dry season, bringing little precipitation. As the southwest monsoon incurs into the basin starting from early May, the discharge rises and reaches its peak in the late monsoon season in October – November; then falls and reaches its minimum in April (MRC 2005). The Mekong's average annual discharge is about 460 km^3 (MRC 2010a). With respect to the components of the Mekong discharge, the Mekong's left bank tributaries located in Laos contribute to the largest (55%), governed by high precipitation in this area; and the upper MRB in China contributes to 16%. In addition, glacial melting water only contributes to 0.1% of the annual mean discharge, because of the small

coverage of glacier in the basin (about 316.3 km^2) (Eastham et al. 2008).

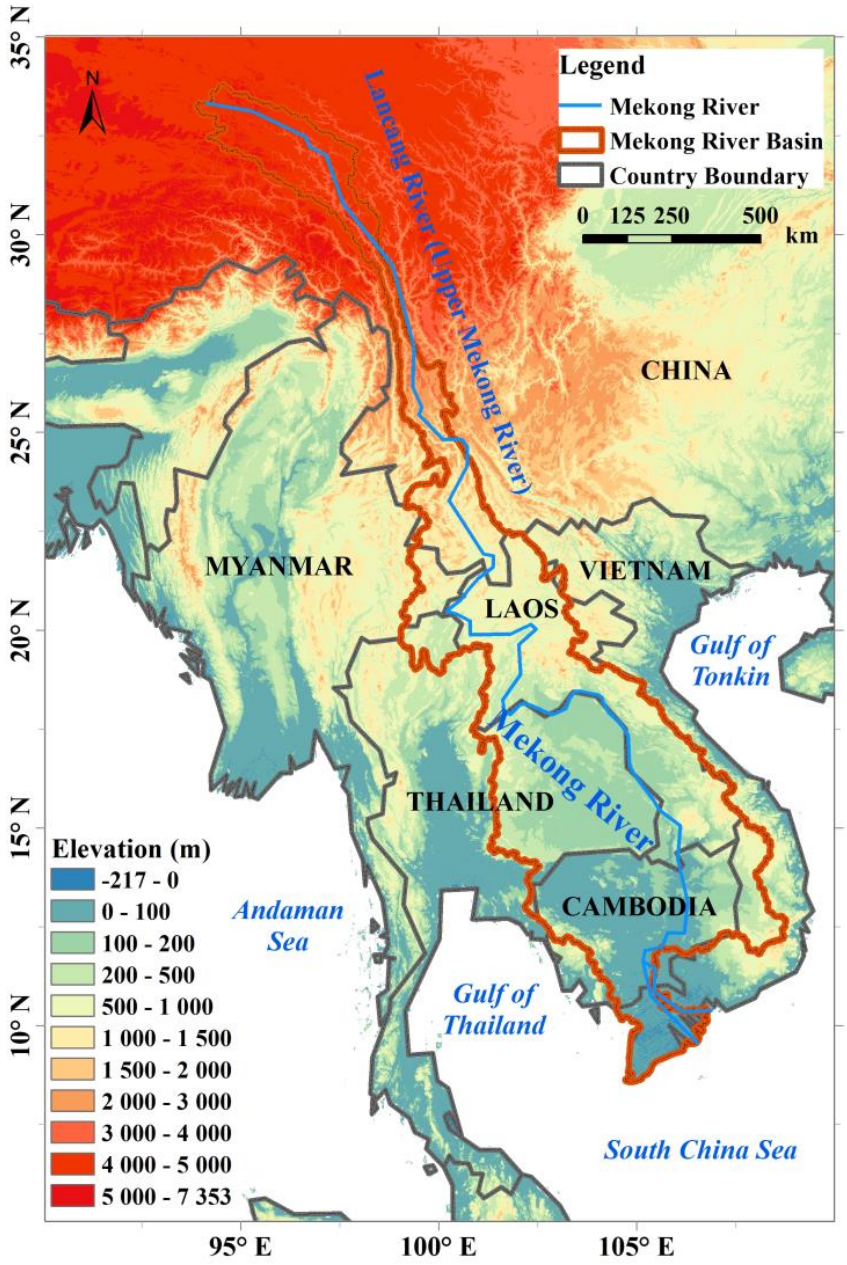

Figure 3. Terrain map of the Mainland Southeast Asia and Mekong River Basin (modified figure 1 from paper II).

TCs are also a climate factor regulating the Mekong flood regimes (Darby et al. 2013; MRC 2010a). TCs influencing the MRB originate from the South China Sea, Western North Pacific (MRC 2007) and North Indian Ocean / Bay of Bengal (Ng and Chan 2012). Among them, Western North Pacific and South China Sea are the primary source oceans; and Western North Pacific is the ocean basin with the greatest

TC activity, having about 30% of global TC occurrence (Peduzzi et al. 2012). TCs usually make incursion into the MRB through Vietnam coastline (MRC 2007) (Figure 4).

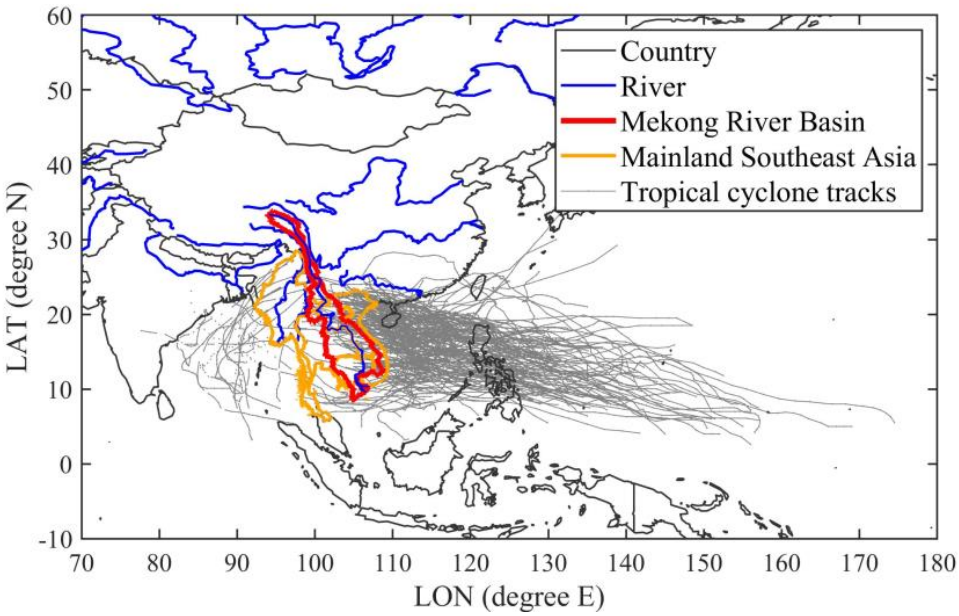

Figure 4. Tracks of tropical cyclones landfall in the Mekong River Basin in 1983 – 2016 (Data source: International Best Track Archive for Climate Stewardship, IBTrACS, https://www.ncdc.noaa.gov/ibtracs/ (Knapp et al. 2010)).

The MRB area has about 70 million population, with 60 million of them living in the lower MRB (part of the following countries: Cambodia, Laos, Myanmar, Thailand, and Vietnam). The lower MRB countries have substantially eradicated extreme poverty and hunger in the past decades, but challenges still exist, as 24% of the regional population are considered below the poverty line (ASEAN 2017; MRC 2011). Despite the regional economic development over the past years, the lower MRB countries are still poor, especially Cambodia, Laos, and Myanmar (ASEAN 2017). 75% of the basin's population settle in rural areas, and many of them live under poor conditions with limited access to clean water and sufficient food (MRC 2010a). The basin's economy is highly dependent on natural resources. Specifically, over 70% of the locals live out of agriculture (MRC 2011). With respect to TCs, the MRB lacks infrastructure to sufficiently cope with the destructive flooding and storms, neither have the local communities sufficient supplies for restoration from natural hazards (ADB 2009; ASEAN 2017; MRC 2010b, 2011). TCs and associated floods can also destroy the farmlands leading to food insecurity. As such, TCs, food insecurity, and

poverty are strongly linked. Thus, the MRB is vulnerable to the challenges from TCs.

2.2 Tropical Cyclones and Impact

2.2.1 Tropical Cyclones

A TC is defined as a non-frontal synoptic-scale low pressure system originating over tropical or subtropical waters with organized convection and definite cyclonic surface wind circulation (Frank 1977; Henderson-Sellers et al. 1998). TCs derive energy primarily from evaporation over the warm ocean and associated condensation in convective clouds concentrated near the center (Henderson-Sellers et al. 1998). As TCs move over land, they decay because of the absence of substantial surface enthalpy sources (Emanuel 2006; Walsh et al. 2016). The formation of TCs occur at locations at least 5° latitude away from the equator, requiring pre-existing disturbances and environmental support for active deep convections (such as warm sea surface temperature [at least 26.5°C to a depth of 60 m], moist mid-troposphere, and low vertical wind shear) (Gray 1968; WMO 2017).

TC structure consists of a rain-free eye, an eyewall, and spiral rainbands (Wang 2012). The TC eye is a calm area that can be as small as 5 km in radius; the strongest winds are near the eyewall that is an indicator of the storm's intensity; and heavy rainfall used to occur at the eyewall and rainbands (Frank 1977; WMO 2017). The size of TCs varies and also during their stages, ranging from 100 to 1000 km in radius (Wang 2012). Based on the intensity (i.e., maximum wind speed [MWS]), TCs are classified into three main groups: tropical depressions (< 34 knots, 1 knot ≈ 0.51 m s^{-1}), tropical storms or tropical cyclones (34 – 63 knots), and a third group of more intense storms (≥ 64 knots), whose name depends on the origin region: typhoons (Western North Pacific), hurricanes (Northeast Pacific Basin, or North Atlantic), and severe tropical cyclones (Indian Ocean, or South Hemisphere) (WMO 2017).

As a main source of TCs influencing the MRB, the Western North Pacific is the world's most active ocean basin, because of the favorable conditions associated with the active Madden–Julian oscillation and equatorial waves (Camargo et al. 2009; Henderson-Sellers et al. 1998; Molinari and Vollaro 2013; Schreck et al. 2012). However, TC activity is also associated with large-scale atmospheric circulations and thermodynamic structure of the atmosphere modulated by ENSO (Elsner and Liu 2003; Ng and Chan 2012; Walsh et al. 2016) and PDO

(Camargo et al. 2010; Goh and Chan 2010; Wang et al. 2013). For instance, strong ENSO events can substantially influence the TC activity in the Western North Pacific that change the seasonal frequency of TC formation at different locations (Elsner and Liu 2003; Wang and Chan 2002; WMO 2017). Besides, ENSO has impacts on the moving tracks of TCs (Elsner and Liu 2003; Wang and Chan 2002). During El Niño years, larger number of northwestward-path TCs occurs, resulting in a smaller number of straight-moving TCs, which can potentially influence the MRB (Elsner and Liu 2003). PDO also has similar impact on TC path shifting, and positive (negative) PDO phase is less (more) favourable for TC formation (Goh and Chan 2010).

2.2.2 Tropical Cyclones Impact

TCs are one of the most disastrous natural hazards in the world (Peduzzi et al. 2012), that have caused about 10,000 deaths and 25 billion USD worth of damages per year worldwide between 1985 and 2018 (CRED 2019). Originating from the warm humid ocean surface, TCs often bring heavy rainfall in a short time period (Emanuel 2008), accompanied by destructive wind storms (Mendelsohn et al. 2012), both of which can affect large areas both inland and coast (Rappaport 2014; Villarini et al. 2014; Zhou and Matyas 2017). The predominant deaths caused by TCs are not the associated strong winds but the rainfall-induced floods (Hu et al. 2018; Jonkman et al. 2009; Rappaport 2014). On average, TCs caused about 14 floods per year globally in 1985 – 2018, contributing to 10.4% of all the occurred floods (Brakenridge 2019). Meanwhile, about 45.1% of the flood-caused deaths are associated with the TC induced floods. Such impacts indicate the devastating impacts of TCs (Rappaport 2014).

Historically, TC events have caused many extreme floods in the MRB. For example, extreme TC Nargis with an intensity of 116 knots made landfall in Myanmar in 2008 and induced extreme wind, rainfall, and floods that caused 136,000 cases of deaths (MRC 2015). Five unprecedented sequences of tropical storms (namely Haima, Nock-Ten, Haitang, Nesat, and Nalgae) caused exceptional historical flooding in the year 2011 in Thailand, damaging agriculture, industry, economy, society and other sectors (Haraguchi and Lall 2015; MRC 2014). TCR can partly cause the second peak of seasonal streamflow in the Mekong River during the late monsoon season (i.e., September – October), when the seasonal discharge is already high (MRC 2010a; Nguyen 2008; Räsänen and Kummu 2013; Takahashi and Yasunari 2008). Intense TCs are a major determinant in the development of

regional flood events in the MRB (Chhin et al. 2016; MRC 2015). It is worth mentioning that TCs can be beneficial for the MRB by supplying water to local areas and enacting river sediment mobilizing downstream, which is very important for the subsiding Mekong Delta in particular (Darby et al. 2013, 2016). The river delta is undergoing subsidence (~1.6 cm $year^{-1}$) and sea level rise (Erban et al. 2014). This is however out of the scope of this thesis, so it will not be discussed here.

2.3 Research Gaps

Prior investigations have estimated the change in TCs and TCR in the MRB at multi-regions across MSEA (Chhin et al. 2016; Nguyen-Thi et al. 2012a,b; Takahashi et al. 2015; Takahashi and Yasunari 2008), yet rare are studies that have been carried out on a long-term climatology of TCs and TCR. Moreover, past studies showed that 90% of the mortality by TCs were caused by drowning due to storm surges and floods in the MRB (Hu et al. 2018; Rappaport 2000, 2014), and TC induced floods have caused deaths accounted for over 80% of total deaths due to floods in Laos and Myanmar (Hu et al. 2018). In spite of the devastating impact of TC induced floods on the MRB, impacts of TC associated floods have been primarily assessed in Vietnam (Balica et al. 2014; Chau et al. 2013) and Thailand (Gale and Saunders 2013; Haraguchi and Lall 2015), but seldomly focused on the MRB. In addition, TC intensity and rainfall rates would most likely increase under climate warming in the 21st century, prominently in the Western North Pacific (Emanuel 2013; Knutson et al. 2015; Walsh et al. 2015), which may result in increasing risk of TCs in the MRB. However, little is known about how future climate warming are likely to affect TCs in the MRB. Considering the disastrous impact of TCs in the MRB, quantitative assessment of TC associated rainfall, floods and their impacts in the past is thus needed for the region. Estimating future changes of TC intensity in the MRB is necessary to increase the resilience of the MRB, as TCs are a threat to the wellbeing of local inhabitants. In addition, accurate precipitation data is fundamental to such studies, but the sparsely and unevenly distributed ground-based rain gauges in the basin are not able to monitor the comprehensive spatiotemporal features of rainfall (Lauri et al. 2014; Lutz et al. 2014; Wang et al. 2016).

2.4 Aims

Given the overarching research needs, this thesis evaluates the existing precipitation datasets for the MRB in assisting the selection of

precipitation data for further study, investigates changes in TCs and the associated rainfall and floods, and estimates future change in TC intensity in the MRB. The overall aim is to contribute to the current understanding of changes of TCs and associated extreme wind, rainfall, and floods' impacts on the MRB. The outcomes will enable an improved understanding of TC impact on humans. It will support for future mitigation and adaptation for societies under climate change.

The four objectives of this thesis are:

i) to assess the reliability of available gridded precipitation data (paper I);
ii) to examine the climatology of landfalling TCs and the associated rainfall (paper II);
iii) to assess the spatiotemporal characteristics of TC induced floods and estimate their impacts (paper III);
iv) to estimate the future change in TC intensity (paper IV).

3 Data and Methods

Research included in this thesis focus on the MRB (paper I, II, and IV) and the lower MRB countries – MSEA (paper III). The studying time periods concentrate on the recent decades from the 1980s, but they slightly vary among researches depending on the available data. Specifically, the time period is 1998 – 2007 in paper I, 1983 – 2016 in paper II, 1985 – 2018 in paper III, and 1981 – 2000 and 2081 – 2100 in paper IV, respectively. Paper I assesses the reliability of available gridded precipitation data to provide evidences for the selection of precipitation data for TCR study in paper II. Paper II applies TC best track and PERSIANN-CDR precipitation data to investigate changes in TCs and TCR in the MRB. As TCs carrying heavy rainfall are prone to trigger floods, this thesis investigates the spatiotemporal characteristics of TC induced floods and estimates their associated impacts on society in the MSEA in paper III. Paper IV estimates the future change in TC intensity under the Representative Concentration Pathway (RCP) 8.5 scenario in the MRB, in order to raise the awareness of potential climate extremes mitigation and adaptation measures.

3.1 Data

3.1.1 Precipitation Datasets

The precipitation datasets used in this thesis consist of an interpolated ground-based observation dataset: the Asian Precipitation – Highly Resolved Observational Data Integration Towards Evaluation of Water Resources (APHRODITE, paper I) (Yatagai et al. 2012), two satellite products: the Tropical Rainfall Measuring Mission post-real-time research products, version 7, 3B42v7 (TRMM 3B42, paper I) (Huffman et al. 2007) and the Precipitation Estimation from Remotely Sensed Information using Artificial Neural Networks—Climate Data Record (PERSIANN-CDR, paper I and II) (Sorooshian et al. 2000), and three reanalysis products: the Climate Forecast System Reanalysis (CFSR, paper I) (Saha et al. 2010), the European Centre for Medium-Range Weather Forecasts interim reanalysis (ERA-Interim, paper I) (Dee et al. 2011), and the Modern-Era Retrospective analysis for Research and Applications Version 2 (MERRA2, paper I) (Gelaro et al. 2017). Details of the datasets can be found in Table 1.

In paper I, the APHRODITE is chosen as the reference data for evaluation as it is developed based on a dense network of rain gauge data and has incorporated a quality control (Tanarhte et al. 2012;

Yatagai et al. 2012). Furthermore, the APHRODITE is treated as a "ground truth" in many previous evaluations of gridded precipitation datasets over the monsoon-affected Asia (Sidike et al. 2016; Sohn et al. 2012; Tan et al. 2017).

Table 1. Global precipitation datasets used in the Mekong River Basin study (modified Table 2 from paper I).

Type	Product	Temporal coverage	Spatial coverage	Spatial resolution	Temporal resolution	Reference
Gauge interpolation	APHRODITE	1951-2007	Eurasia 15S-55N, 60E-150E	0.25°* 0.25°	Daily	Yatagai *et al.* (2012)
Reanalysis	CFSR	1979-2011	Global	0.5°* 0.5°	6-hourly	Saha *et al.* (2010)
	ERA-Interim	1979-present	Global	0.75°* 0.75°	6-hourly	Dee *et al.* (2011)
	MERRA2	1980-present	Global	0.5°* 0.625°	1-hourly	Gelaro *et al.* (2017)
Satellite	PERSIANN-CDR	1983-present	60°N-60°S	0.25°* 0.25°	Daily	Sorooshian *et al.* (2014)
	TRMM 3B42	1998-2019	50°N-50°S	0.25°* 0.25°	3-hourly	Huffman *et al. (*2007)

3.1.2 Tropical Cyclone Best Track Dataset

The observed TC track data, so called "best track" data, is based on all available data consisting of ship, surface, and satellite observations (Knapp et al. 2010). In this thesis, the best track data is obtained from the International Best Track Archive for Climate Stewardship (IBTrACS, https://www.ncdc.noaa.gov/ibtracs/index.php), which provides the most complete and reliable worldwide collection of historical TC best track dataset. The IBTrACS contains information about each individual storm at a 6-hour interval, such as the name of the storm, position of the storm center, type of storm, maximum sustained wind speeds (knot), and minimum central pressure (hPa) (Knapp et al. 2010). In the archive, the best track data from Regional Specialized Meteorological Centers Tokyo between 1983 and 2016 is used for paper II, which investigates all the TCs that have affected the MRB formed in source oceans (Western North Pacific, South China Sea and North Indian Ocean).

3.1.3 GCM Simulations

Large-scale flows, such as winds at 850 and 250 hPa, temperature and relative humidity at 600 hPa, and sea surface temperature, from five global climate models (GCMs) provided by the Coupled Model Intercomparison Project Phase 5 (CMIP5) (Taylor et al. 2012) are used

for simulating TCs influencing the MRB in 1981 – 2000 and 2081 – 2100 (under RCP 8.5 scenario) (Emanuel et al. 2008). The GCMs consist of the GFDL-CM3, HadGEM2-ES, IPSLCM5A-LR, MIROC5, and MPI-ESM-MR; abbreviated as GFDL5, HadGEM5, IPSL5, MIROC5, and MPI5, respectively. The horizontal resolutions and other details of these GCMs can be found in Table 2. Future projections under the high emission RCP8.5 scenario is the "worst case" scenario of future TC activity. With this projection, the extreme results from this thesis can be seen as a warning for the "worst", if humans take "business as usual" development path (IPCC 2013; van Vuuren et al. 2011).

Table 2. List of five the Coupled Model Intercomparison Project Phase 5 (CMIP5) global climate models used for the downscaling approach (modified Table S1 from paper IV).

Acronym	Modelling center	Institute ID	Model name	Average horizontal resolution	Reference
GFDL5	NOAA Geophysical Fluid Dynamics Laboratory	GFDL	CM3	2.5° * 2.0°	Donner *et al.* (2011)
HadGEM5	Met Office Hadley Center	MOHC	HadGEM2-ES	1.875°* 1.24°	Collins *et al.* (2011)
IPSL5	L'Institut Pierre-Simon Laplace	IPSL	IPSL-CM5A-LR	3.75°* 1.875°	Dufresne *et al.* (2013)
MIROC5	Atmosphere and Ocean Research Institute (The University of Tokyo), National Institute for Environmental Studies, and Japan Agency for Marine-Earth Science and Technology	MIROC	MIROC5	1.4°* 1.4°	Watanabe *et al.* (2010)
MPI5	Max Planck Institute for Meteorology	MPI	MPI-ESM-MR	1.875°* 1.865°	Giorgetta *et al.* (2013)

3.1.4 Climate Indices

Since TC activity is related to ENSO (Elsner and Liu 2003; Ng and Chan 2012; Walsh et al. 2016) and PDO (Camargo et al. 2010; Goh and Chan 2010; Wang et al. 2013), links between these two large-scale atmospheric circulations and TCs influencing the MRB are investigated in paper II. The ENSO index is obtained from the Golden Gate Weather Services (http://ggweather.com/enso/oni.htm) and the Climate Prediction Center from National Oceanic and Atmospheric Administration (NOAA, http://origin.cpc.ncep.noaa.gov/products/analysis_monitoring/ensostuf

f/ONI_v5.php). Three months' mean ENSO index (December – February) is used for representing ENSO index in each year (Diamond et al. 2013; Elsner and Liu 2003). The PDO index is obtained from the Physical Sciences Division at the Earth System Research Laboratory, NOAA (http://www.esrl.noaa.gov/psd/gcos_wgsp/Timeseries/PDO/index.html).

3.1.5 Floods Data

The evaluation of spatiotemporal impacts of floods in paper III is based on the Dartmouth Flood Observatory Global Active Archive of Large Flood Events (http://floodobservatory.colorado.edu/Archives/index.html). This data archive records information about any floods from 1985 with significant damages or fatalities such as location, duration, affected population, geographic flood extents, flood magnitude, and main causes (Brakenridge 2019). Since this thesis is interested in estimating the impact from the TC induced floods, two groups of floods are investigated: floods by all various possible causes (ALLFloods), and TC induced floods (TCFloods).

3.1.6 Gridded Population Data

The estimation of flood impact is assisted by the gridded population data to normalize flood induced impact. Population data is derived from the National Aeronautics and Space Administration (NASA) Socioeconomic Data and Applications Center (SEDAC): Global Population Count Grid Time Series Estimates, v1 (GPCv1) (CIESIN 2011, 2017), and Gridded Population of the World, Version 4 (GPWv4): Population Count, Revision 11 (CIESIN 2018). Regarding the gridded population data's temporal interval, GPCv1 provides every 10 years in 1970 – 2000; and GPWv4 provides every 5 years in 2000 – 2020.

3.1.7 Flood Protection Standard Database

To explore drivers of the spatial heterogeneity of flood impacts, the flood protection standards database – FLOodPROtection Standards (FLOPROS) (Scussolini et al. 2016) is employed. This database contains information of actual, enforced flood protection on different spatial scales, in particular structural measures of flood protection such as dikes, levees, and reservoirs. The information on flood protection measures is presented as flood return periods which is associated with the estimation of probability of flood events. In other words, flood return periods are defined as the inverse of the annual exceedance probability

of flood events (Bangalore et al. 2019). The higher flood return periods indicate higher flood protection measures to prevent from flood risk.

3.2 Methods

3.2.1 Statistical Analyses

Several commonly used statistical methods are employed in the thesis, such as the Pearson's correlation coefficient (*r,* paper I and II), partial correlation coefficient (paper II), relative bias (RBS, paper I), normalized root mean-square error (NRMSE, paper I), and Nash–Sutcliffe coefficient of efficiency (NS, paper I) (Moriasi et al. 2007; Nash and Sutcliffe 1970). A score-based method, Rank Score (Fu et al. 2013), is then employed to achieve the purpose of evaluating an overall performance of each data, based on the results of above listed assessment statistical methods (*r*, RBS, NRMSE, and NS). Taylor diagrams are used to visualize the statistic performance (Taylor 2001). For trend analyses, Sen's slope (Sen 1968) and Mann-Kendall (Kendall 1938) are applied, with a confidence level of 95% ($p < .05$) (paper I, II, and III). Sen's and Mann-Kendall methods are broadly used in hydroclimate time series data analyses (Feng and Zhou 2012; Wu et al. 2016).

3.2.2 Definition of Tropical Cyclone Associated Rainfall

Previous studies indicated that most of the TC associated rainfall (TCR) take place within a radius of 500 km (Jiang and Zipser 2010; Khouakhi et al. 2017; Lin et al. 2015). This thesis defines the TCR as any rainfall occurred inside an area centered with the TC center alongside its track (Jiang and Zipser 2010; Khouakhi et al. 2017; Zhang et al. 2018). This area is a square box with a half side length of 500 km (i.e., 1,000 km in diameter) (in paper II). Since the precipitation data employed in this study is PERSIANN-CDR, the TC center of all the TCs influencing the MRB is aggregated from a 6-hour into daily interval to match the temporal resolution of precipitation data. With this definition, TCR is then computed along the daily TC track's center (Figure 5). Spatial patterns of monthly, seasonal, and annual TCR are calculated, as well as the basin scale temporal mean TCR. The spatiotemporal mean total precipitation is also assessed, in order to evaluate the contribution of TCR (TCR contribution to total precipitation, abbreviated as TCRC, in %) at each period of interest.

Extreme precipitation indices are employed to analyze the influence of TCR on extreme precipitation, namely, the R20mm (days of heavy

precipitation rate ≥ 20 mm day^{-1}) and R50mm (days of extremely heavy precipitation rate ≥ 50 mm day^{-1}) (Donat et al. 2013; Imbach et al. 2018; Lestari et al. 2016). The ratio of extreme precipitation days caused by TCs to annual total precipitation is also measured.

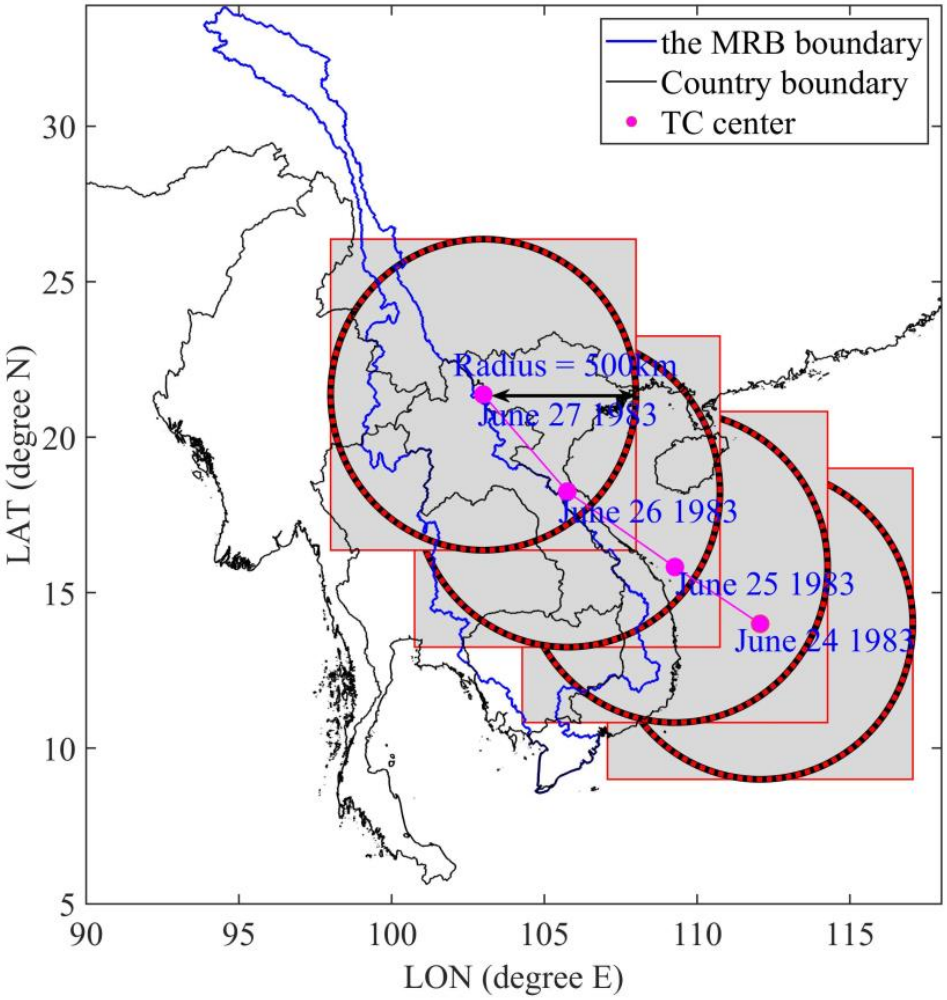

Figure 5. An illustration of spatial coverage of a tropical cyclone on 24th - 27th June 1983 across the Mekong River Basin. The red dash circle is the range of 500 km radius of the tropical cyclone centre; and the rainfall that occurs within the shaded red solid square area is considered as tropical cyclone rainfall in this study (modified Figure 1 from paper II).

3.2.3 Normalization of Flood Loss

Normalizing flood induced impact on human live loss and displacement is important because, for example, changes in flood mortality can be attributed by increased population density instead of flood intensity over time and space (Jonkman 2005; Neumayer and Barthel 2011). Here,

the thesis first estimates annual gridded population by intermediate years' interpolation using the annual exponential growth rate (Balk et al. 2006; Doxsey-Whitfield et al. 2015). The potentially influenced population of floods is then estimated to normalize flood impacts on humans regarding displacement and mortality rates, defined as the total population within the corresponding flood spatial extent (paper III). Normalized flood mortality and displacement rates are measured as follows (Cunado and Ferreira 2015; Jonkman 2005; Neumayer and Barthel 2011):

$$Mortality\ rate = log\left(1 + \frac{Number\ of\ Dead}{Potentially\ influenced\ population\ per\ million\ persons}\right) \quad \text{eq. (1)}$$

$$Displacement\ rate = log\left(1 + \frac{Number\ of\ Displaced}{Potentially\ influenced\ population\ per\ million\ persons}\right) \quad \text{eq. (2)}$$

3.2.4 Tropical Cyclone Downscaling Simulations

GCMs tend to underestimate TC activity constrained by their coarse horizontal resolutions (~100 km) (Camargo 2013; Zhang et al. 2017a). Common dynamic downscaling simulations using regional climate models do not have sufficient horizontal resolutions (~10 – 50 km), nor are they cost-efficient to perform (Emanuel 2008; Emanuel et al. 2008). A downscaling technique developed by Emanuel *et al.* (2006, 2008) is able to overcome the above-mentioned drawbacks (Emanuel et al. 2008). Briefly, this technique first randomly distributes weak warm-core vortices (25 knots) in space and time. A majority of these vortices will dissipate due to the unfavorable environmental conditions failing to form TCs. The seed vortices are then propagated according to the beta-and-advection model along the ambient large-scale flows from GCMs, generating a large number of synthetic TCs (~10^3). The large-scale flows are constrained to have compatible statistics agreed with historical observations. A simpler embedded model (Coupled Hurricane Intensity Prediction System) is finally run along the simulated synthetic TCs tracks to estimate their intensity. The Coupled Hurricane Intensity Prediction System model is phrased in angular momentum coordinates, yielding a high radial resolution of the TC's eyewall region, which is critical to determining the TC intensity (Emanuel 2006, 2008; Emanuel et al. 2006). The technique can also be used for future TC activity projection (Emanuel 2013; Lin et al. 2012). Prior studies have proved the capability of this technique in simulating TCs and applications in risk assessment (Emanuel 2017a; Lin et al. 2012; Mendelsohn et al. 2012). Interested readers can refer to Refs Emanuel *et al.* (2006, 2008), which offer more in-depth descriptions of this downscaling technique.

The downscaling technique is applied to simulate TC activity influencing the MRB both at a historical period (1981 – 2000) and future projection (2081 – 2100, RCP8.5 scenario), using large-scale flows from the five GCMs employed from CMIP5 (Taylor et al. 2012). These GCMs meet the requirements for the technique (Emanuel et al. 2006) and have good continuity between historical and future projections (Emanuel 2013, 2017a). Regarding all the generated TCs, only those with intensity greater than 30 knots passed a predefined MRB boundary are treated as the TCs influencing the MRB. Simulation of the historical TCs using GCMs is first carried out. The annual frequency of TCs from each GCM is calibrated to match the best track data derived from the Joint Typhoon Warning Center (JTWC, http://www.metoc.navy.mil/jtwc/jtwc.html), obtaining a calibration constant. The future simulation for each GCM is then completed to estimate for example, the annual frequency of TCs in 2081 – 2100, using the calibration constant under the RCP8.5 scenario.

4 Results and Discussions

4.1 Evaluation of Gridded Precipitation Datasets

In paper I, assessment reveals that most of the investigated datasets agree with the general precipitation patterns in the MRB for 1998 – 2007 in comparison with the APHRODITE reference data. MERRA2 and TRMM 3B42 perform the best regarding statistical performance at all the temporal scales (annual, wet season, dry season, and daily) (Figure 6). These two datasets show relatively smaller bias and higher correlation coefficients. PERSIANN-CDR lists as third in terms of statistical performance. In addition, MERRA2 and ERA-Interim have higher similarities to APHRODITE in resembling the probability density distribution of daily mean precipitation.

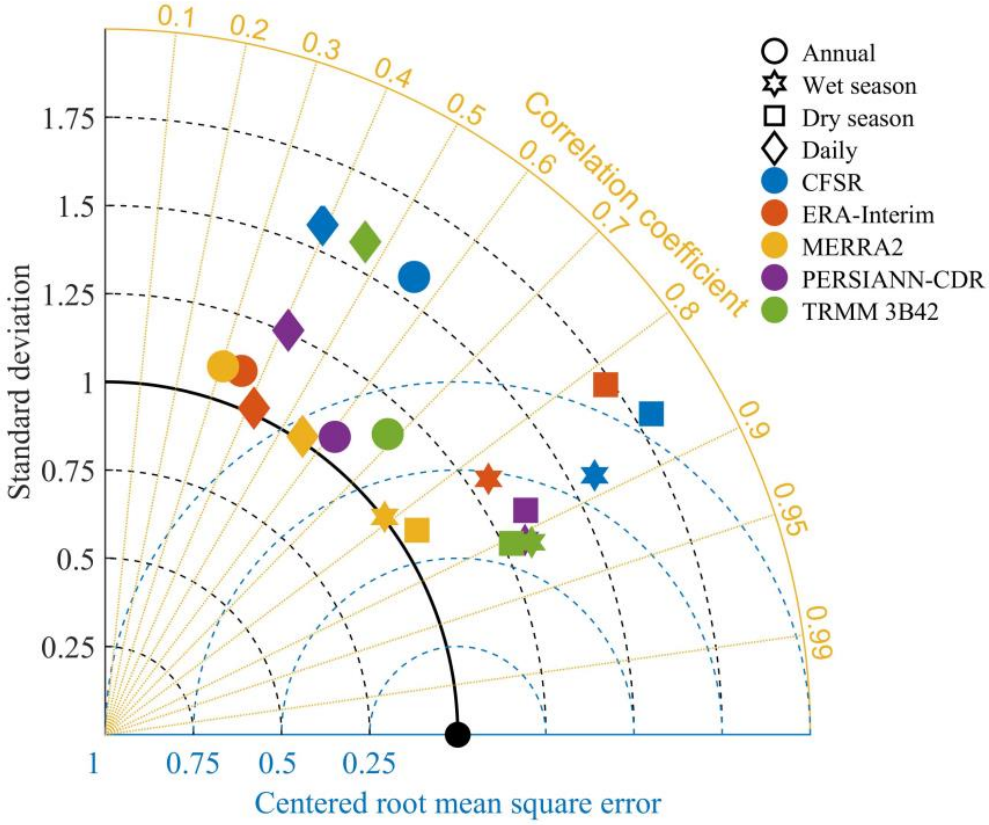

Figure 6. Taylor diagram of precipitation in the Mekong River Basin for 1998 – 2007, with shapes and colours indicating temporal scale and investigated data, respectively (Figure 5 in paper I).

Regarding spatial variability, TRMM 3B42 well captures the spatial distribution of precipitation (Figure 9 and 10 in paper I) when compared with APHRODITE. PERSIANN-CDR also shows high spatial variability

with the reference data. CFSR is reasonable at resembling the spatial variability of precipitation. However, it overestimates the magnitude and statistical significance of negative trends, particularly in the lower MRB. Both MERRA2 and ERA-Interim present inconsistent spatial variability compared with the APHRODITE.

Overall, the satellite products (TRMM 3B42 and PERSIANN-CDR) perform better in capturing the precipitation of APHRODITE than reanalysis products on both spatial and temporal scales across the MRB; and TRMM 3B42 is superior to PERSIANN-CDR. As to the reanalysis products, MERRA2 is better at resembling the precipitation's temporal variability; however, it somehow underestimates the precipitation. Although CFSR and ERA-Interim largely overestimate the precipitation, they are good at capturing the spatial variability of precipitation, and daily precipitation probability, respectively.

Divergent performances of the investigated datasets in the assessment root in their individual unique remote sensors and numerical models (Decker et al. 2012; Wang and Zeng 2012). A reanalysis uses a background forecast physical model and assimilates available observations to simulate a state of atmosphere (Betts et al. 2006; Sun et al. 2018; Wong et al. 2017). Accuracy of the estimated precipitation depends on the assimilated observations, model parameterizations, and forecast-analysis systems (Betts et al. 2006). The precipitation correction algorithm of MERRA2 can be a reason for its good performance in estimating precipitation temporal variability (Gelaro et al. 2017; Reichle et al. 2017a,b); but the exclusion of land surface analysis may lead to unreliable spatial distribution of precipitation (Reichle et al. 2017a). Lauri et al. (2014) also indicates relatively poor performances of CFSR and ERA-Interim.

Since satellite precipitation products have the advantages of consistent spatial continuity and high temporal frequency (Ashouri et al. 2015; Nasrollahi et al. 2013), they generally capture better spatiotemporal variability of precipitation than reanalysis products (Rana et al. 2015; Seyyedi et al. 2015; Tan et al. 2017). TRMM 3B42 combines high-quality infrared and passive microwave measurement satellite information and gauge analyses to estimate precipitation, with a bias adjustment using the latest Global Precipitation Climatology Centre data (Huffman et al. 2007; Huffman and Bolvin 2012). As the passive microwave measurement satellite observations are limited in the pre-1997 period, they hinder the development of long-term satellite-based precipitation products, because most of the existing satellite

precipitation products, for example TRMM 3B42, depend on the input of these observations (Ashouri et al. 2015). With the help of an artificial neural network model, PERSIANN-CDR is developed primarily using the global archived infrared satellite information, so that it avoids the requirement of passive microwave measurement satellite observations (Ashouri et al. 2015; Huang et al. 2016; Sorooshian et al. 2000). The PERSIANN-CDR has incorporated a bias adjustment using the Global Precipitation Climatology Project monthly precipitation data. The reliabilities on spatial and temporal scales of PERSIANN-CDR and TRMM 3B42 have been proved in pioneering studies (Chen et al. 2013b; Rana et al. 2015; Tan et al. 2017).

To summarize, each precipitation dataset has its pros and cons, fitting different aims of studies. A suitable investigation for the selection of precipitation data is necessary for individual studies. TRMM 3B42 has a short temporal availability from 1998 which is not feasible for long-term climatological studies. PERSIANN-CDR is the only satellite-based global precipitation data available from 1983, allowing a long-term investigation of water cycle (Ashouri et al. 2015). Given the PERSIANN-CDR's good performance and long temporal availability, it is applied for further study of TCR in the MRB in paper II.

4.2 Tropical Cyclones and Their Associated Rainfall

4.2.1 Tropical Cyclones

Paper II shows that 6.2 TCs influenced the MRB for 13 days per year on average between 1983 and 2016 (Figure 7), with a mean MWS of 51.8 knots. About 91% of the TCs were formed in Western North Pacific and South China Sea, and the remaining 9% was from North Indian Ocean / Bay of Bengal. Among the 6.2 TCs, 5.2 of them occurred in monsoon-TC season (June – November). Both annual TC number (-0.1 year^{-1}, $p < .05$) and TC duration (-6.2 hours year^{-1}, $p < .05$) significantly decreased during these years. Overall, there was a decreasing trend in the frequency of TCs influencing the MRB. Additionally, a declining trend was also observed in MSEA in 1951 – 2000 (in September) (Takahashi and Yasunari 2008).

Two possible reasons could explain such a decreasing TC frequency trend. First, TCs influencing the MRB primarily formed in Western North Pacific and South China Sea. Although no clear change in TCs was observed in the Western North Pacific (Liu and Chan 2013; Tao and Lan 2017; Yeh et al. 2010), a shifting flow of TCs from straight-moving to northwestwards was observed for the TCs originated from Western

North Pacific since the 1960s (Lee et al. 2012; Park et al. 2011; Wu et al. 2005). Such a shift resulted in the declining number of TCs entering the South China Sea and influencing the MRB (Lee et al. 2012; Park et al. 2014; Wang et al. 2013). Meanwhile, an enhancement of TC trend existed in East Asia caused by the shift (Chen et al. 2013a; Park et al. 2011, 2014). Second, fewer TCs have formed over the southern South China Sea from 1977 (Park et al. 2014), and a decreasing trend in the post-monsoon TCs existed in the Bay of Bengal since the 1960s (Sahoo and Bhaskaran 2016), which was associated with the increasing sea surface temperature in the tropical Indian Ocean (Wang et al. 2013).

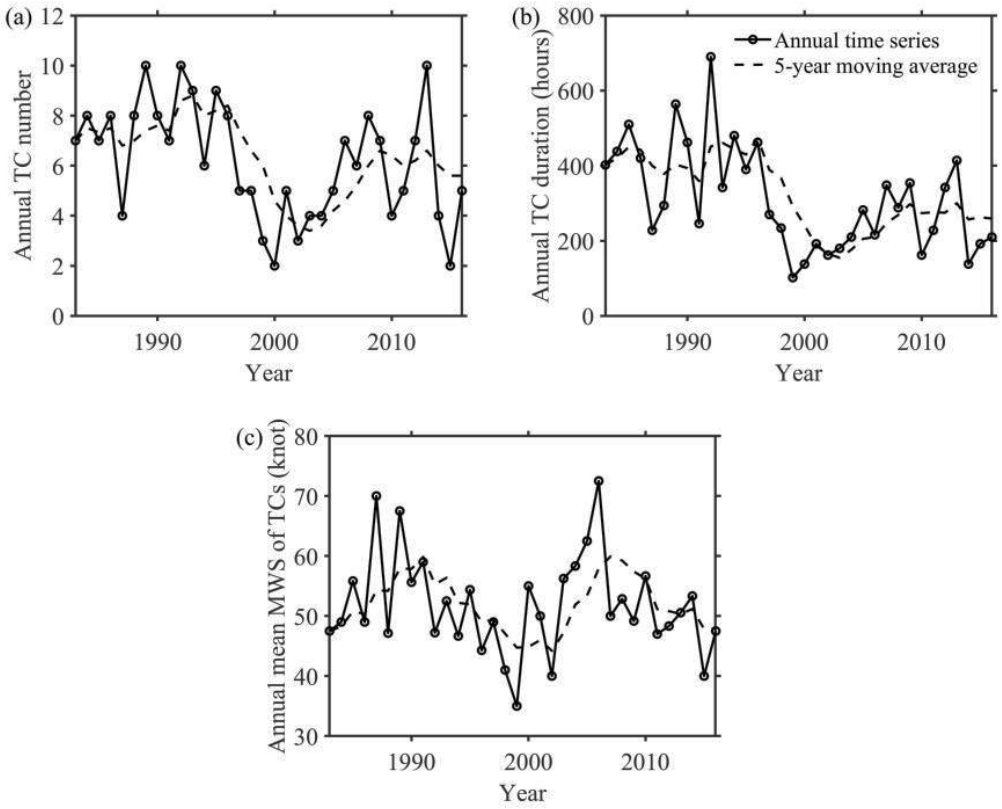

Figure 7. Characteristics of annual tropical cyclone (TC) activity across the Mekong River Basin for 1983 – 2016. (a) TC number; (b) TC duration (in hours); (c) mean maximum wind speed (MWS) of TCs (in knot). Black dash line in each sub-figure is the 5-year moving average (Figure 5 in paper II).

Consistent with previous studies, such as Park *et al.* (2011, 2014), significant correlations between TCR and TC indices were observed (TC number and duration). TC intensity was found correlated with the genesis location of TCs (Park et al. 2011, 2014). Although TC activity closely correlated with ENSO and PDO (Elsner and Liu 2003; Jiang and Zipser 2010; Lee et al. 2012; Walsh et al. 2016), results showed

negative but insignificant correlation coefficient between TC number and ENSO/PDO (Table 1 in paper II). However, the total precipitation was found to significantly correlate with these two circulations.

4.2.2 Tropical Cyclone Associated Rainfall

Regarding the annual distribution, both total precipitation and TCR mainly took place in the monsoon season. The monthly total precipitation peaked in July – August, but TCR peaked in September – October (Figure 8). In addition, the TCR occurred in June – November contributed to 95% of annual TCR. The most active TC season in Western North Pacific (and South China Sea) is June – November with peak months varying between July and October (Camargo and Sobel 2005; Wang and Chan 2002; Wang et al. 2013); and TC landfall in the MRB reaches its peak in September – October (MRC 2015; Nguyen-Thi et al. 2012a). Hence, results from this thesis are consistent with previous studies.

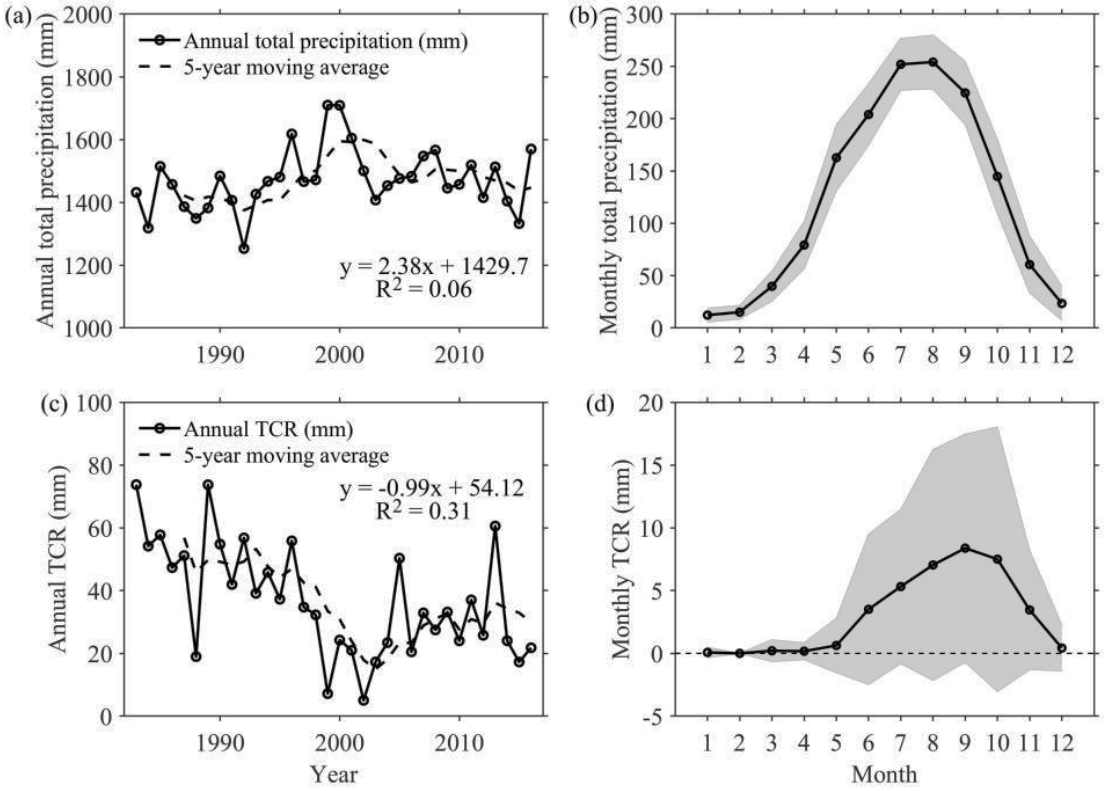

Figure 8. Spatially averaged precipitation (in mm) across the Mekong River Basin for 1983 – 2016. (a) Annual total precipitation; (b) Monthly mean total precipitation; (c) Annual tropical cyclone associated rainfall (TCR); and (d) Monthly mean TCR. Black dash line in (a) and (c) is the 5-year moving average, and the grey shade in (b) and (d) is the range of ±1 standard deviation. Equations shown in (a) and (c) are the linear trend regressions, respectively (Figure 3 in paper II).

Over the MRB, the annual mean total precipitation was about 1,470 mm year^{-1} and the annual mean TCR was 36.7 mm year^{-1} for 1983 – 2016. No clear trend was observed in annual mean total precipitation, but a significant decreasing trend in TCR existed in the MRB during 1983 and 2016 (−1.1mm year^{-1}, $p < .01$). On average, TCR attributed a minor amount of 2.5% to annual total precipitation in the basin (1983 – 2016).

The annual mean total precipitation in the MRB exhibited distinct spatial gradient: increases from northwest to southeast. The annual mean TCR mainly occurred in the lower MRB, with west to east increasing gradient. About 66.6% of the basin area was under the influence of TCR. The lower eastern part of MRB received the maximum precipitation from both annual mean total precipitation and TCR with the amount of 2800 and 330 mm year^{-1}, respectively (Figure 9a, b). TCs landfall in the MRB used to pass Vietnam (MRC 2007, 2015) resulting in the high TC track density concentrated on the eastern lower MRB (Figure 8 in paper II). In regard to the annual mean TCR contribution to the total precipitation (TCRC), its spatial distribution was dominated by TCR, with the maximum TCRC of 12.4% located in the eastern lower MRB (Figure 9c). Contribution of extreme precipitation from TCR also concentrated on the eastern lower MRB (Figure 4 in paper II). Moreover, the TCR is crucial in terms of extreme precipitation, with the maximum contribution of 17.1% for R20mm, and 29.6% for R50mm.

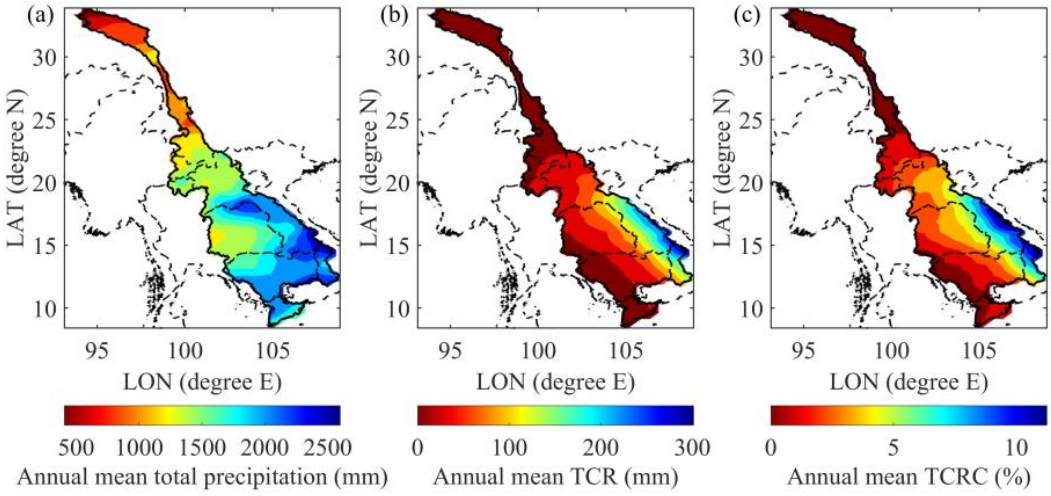

Figure 9. Spatial patterns of annual mean (a) total precipitation (in mm), (b) tropical cyclone associated rainfall (TCR) (in mm), and (c) contribution of TCR to total precipitation (TCRC) (in %) across the Mekong River Basin for 1983 – 2016 (Figure 2 in paper II).

For the short duration but high spatiotemporal concentration of TCs in the eastern lower MRB, TCs landfall in the MRB may potentially induce floods affecting local area by carrying heavy rainfall (Rios Gaona et al. 2018; Zhang et al. 2018). This can be exacerbated when high frequency of TC successions hit the area especially in September, which has higher probability in Southeast Asia than elsewhere in the Tropics (MRC 2015). Results of the large contribution of TCR to extreme precipitation are also evidence of the flooding risk.

4.3 Tropical Cyclone Induced Floods

In paper III, this thesis further investigates the TC impact on floods occurred in the lower MRB countries – MSEA. Similar to TCR, ALLFloods (floods by all possible causes) and TCFloods (TC induced floods) reached their peaks in August – October, and October – November, respectively. These different flood peaks were associated with the timing of monsoon and TC landfall (paper II) (Nguyen-Thi et al. 2012a; Wang and Chan 2002). ALLFloods showed significant increasing trend in 1985 – 2018 (Figure 2 in paper III); no clear trend was found in TCFloods, which could be partly explained by the insignificant trend in landfalling TC intensity (Park et al. 2014) and TCR (in paper II). On average, the annual mean occurrence of TCFloods amounted to 24.6% of ALLFloods. Regarding the trends in flood indices, annual mean flood severities of ALLFloods and TCFloods significantly increased (1985 – 2018), whereas flood-induced mortality (ALLFloods) and displacement rates (ALLFloods and TCFloods) decreased significantly (1988 – 2018) (Figure 4 in paper III). However, abrupt spikes of the TCFloods impact indices occurred in some years marked the extreme influences from uncommon TCFloods events (Doocy et al. 2013).

Spatial distribution of TCFloods was distinct from ALLFloods in the MSEA. ALLFloods scattered over the region as monsoon rainfall is a main cause, which is regulated by the southwest monsoon (Delgado et al. 2010) (Figure 10). TCFloods mostly occurred in the eastern MSEA primarily because of the TC landfall tracks in the region (paper II). Central Vietnam was a focal area of flood occurrence with the highest annual flood frequency of 1.3 $year^{-1}$ and 0.6 $year^{-1}$ for ALLFloods and TCFloods, respectively.

Respecting relative impacts, TCFloods posed higher impacts on humans than the average of ALLFloods on the regional scale. For example, there were higher mortality and displacement rates from TCFloods than ALLFloods at most of the magnitudes during the same

time periods (Figure 11). Higher mortality rate from TCFloods was also found on the national scale, as the ratio of TCFloods mortality to ALLFloods mortality were much higher than the ratio of these two floods' occurrences (Figure 6 in paper III, and Table 3). Among the five countries, Myanmar and Cambodia suffered more from TCFloods than other countries, even though Vetnam had the highest flood occurrence. Specifically, the annual mean of 30.0% contribution from TCFloods occurrence in Vietnam has led to 64.0% of Vietnam's flood mortality, but the annual mean of 8.0% TCFloods occurrence in Myanmar has caused 45.0% of Myanmar's flood mortality.

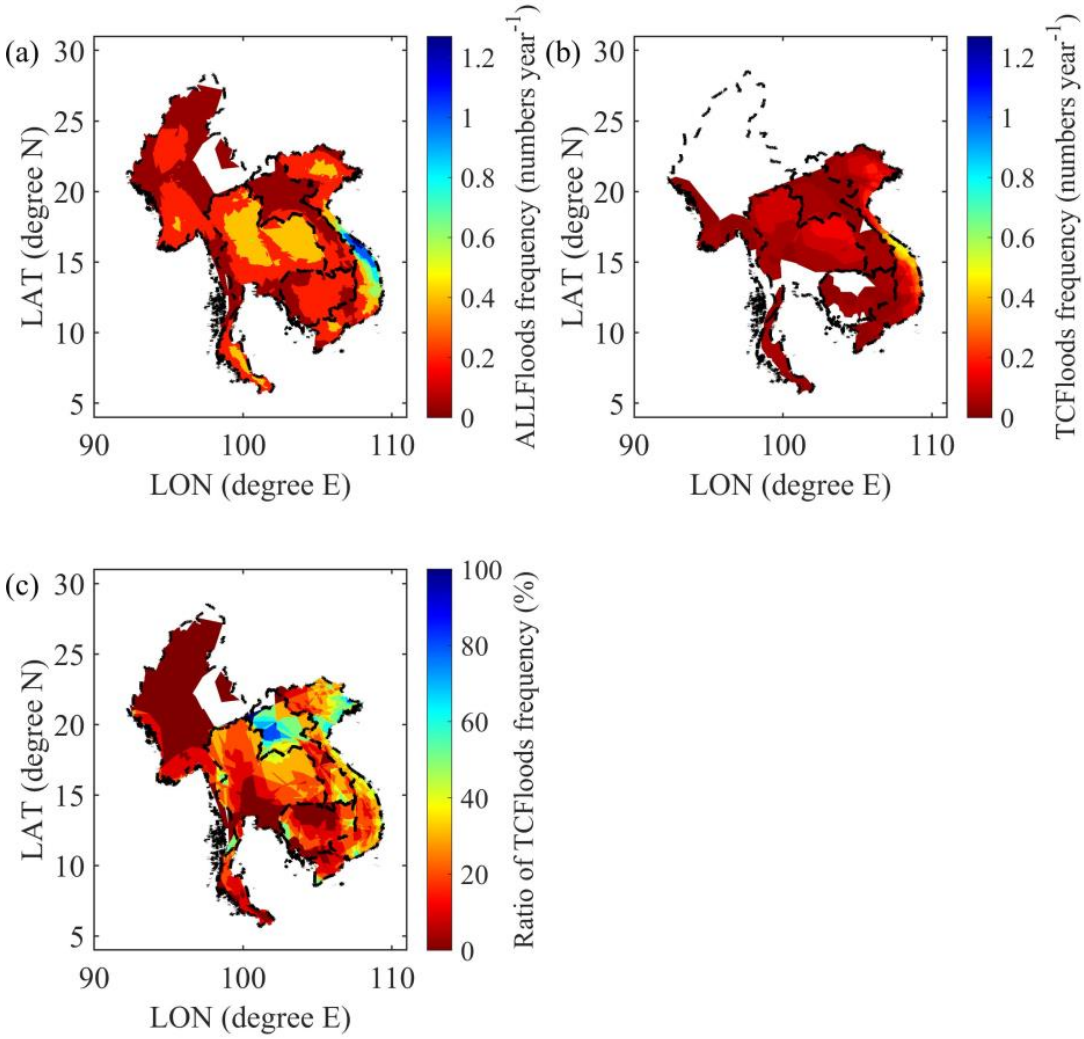

Figure 10. Spatial pattern of annual mean flood frequency in the Mainland Southeast Asia for 1985 – 2018. (a) floods by all causes (ALLFloods), (b) tropical cyclone-induced floods (TCFloods), and (c) ratio of TCFloods frequency to ALLFloods frequency (in %) (Figure 7 in paper III).

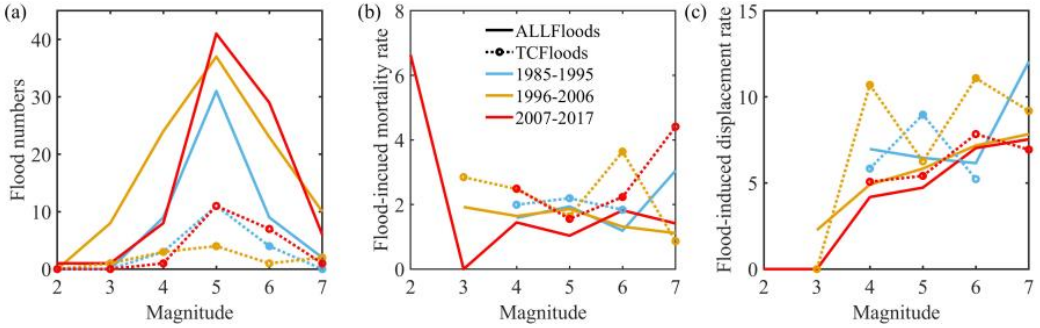

Figure 11. Relationship between flood magnitude and other flood indices by every 11 years: 1985 – 1995, 1996 – 2006, and 2007 – 2017 in the Mainland Southeast Asia. (a) flood numbers, (b) mortality rate, and (c) displacement rate. The blue, orange and red color denote the time period of 1985 – 1995, 1996 – 2006, and 2007 – 2017, respectively. The solid line represents floods by all causes (ALLFloods), and the dashed line with circle marker represents tropical cyclone-induced floods (TCFloods) (Figure 5 in paper III).

Table 3. Statistics of annual mean floods and mortality in riparian countries of the Mainland Southeast Asia for 1985 – 2018. The floods by all causes is abbreviated as ALLFloods, and the tropical cyclone-induced floods is abbreviated as TCFloods. The ratio of TCFloods number to ALLFloods number is calculated, as well as the ratio of TCFloods mortality to ALLFloods mortality (modified Table S2 from paper III).

Countries		Cambodia	Laos	Myanmar	Thailand	Vietnam
Flood number (number per year)	ALLFloods	0.4	0.2	0.8	2.3	3.7
	TCFloods	0.1	0	0.1	0.3	1.1
	Ratio (%)	21.4	16.7	7.7	11.7	29.8
Flood-induced mortality rate	ALLFloods	0.6	0.2	0.6	1.3	1.9
	TCFloods	0.1	0.1	0.3	0.4	1.2
	Ratio (%)	21.9	23.2	45.5	29.3	64.5

Adequate flood protection measures are an important mean to reduce flood risk (Jongman et al. 2014; Palmer 2013; Scussolini et al. 2016). Divergent flood protection standards in the MSEA show spatial heterogeneous flood protection measures implemented to prevent flood risk. Thailand has the highest national mean flood protection standards (17.9 years return period), followed by Vietnam (10.4), Laos (6.8), Cambodia (3.4), and Myanmar (2.2). In fact, Myanmar has basically no flood protection, as natural bank-full discharge can prevent against floods with a 2-year return period (Scussolini et al. 2016). Low/no flood protection standards in Myanmar and Cambodia can be a critical factor to their high flood impacts (Figure 12a). At subnational level, the spatially featured flood protection at areas with high flood occurrence is effective at preventing floods. For example, high flood occurrence areas

in central (Thừa Thiên Huế province) and northern (Hanoi) Vietnam are facilitated with the highest flood protection standards nationwide (up to 120 years return period). Neither Cambodia nor Myanmar have adequate flood protection standards at the subnational level. Overall, all five countries suffer from high magnitude floods.

Joint analysis of flood protection standards and spatial population distribution in 2015 in the MSEA (Figure 12b) further reveals potential challenges for the locals from projected future floods (Hoang et al. 2016) with TC induced floods in particular. Higher flood protection standards have been facilitated in large cities with high population density, e.g., Hanoi in Vietnam, and Bangkok in Thailand. Other highly populated areas however, still lack sufficient flood prevention measures, especially the Mekong Delta, which is facing high risk of floods aggregated by the sea level rise and land subsidence (Erban et al. 2014). Therefore, the flood protection in the MSEA is not yet sufficient to deal with potential flood risk.

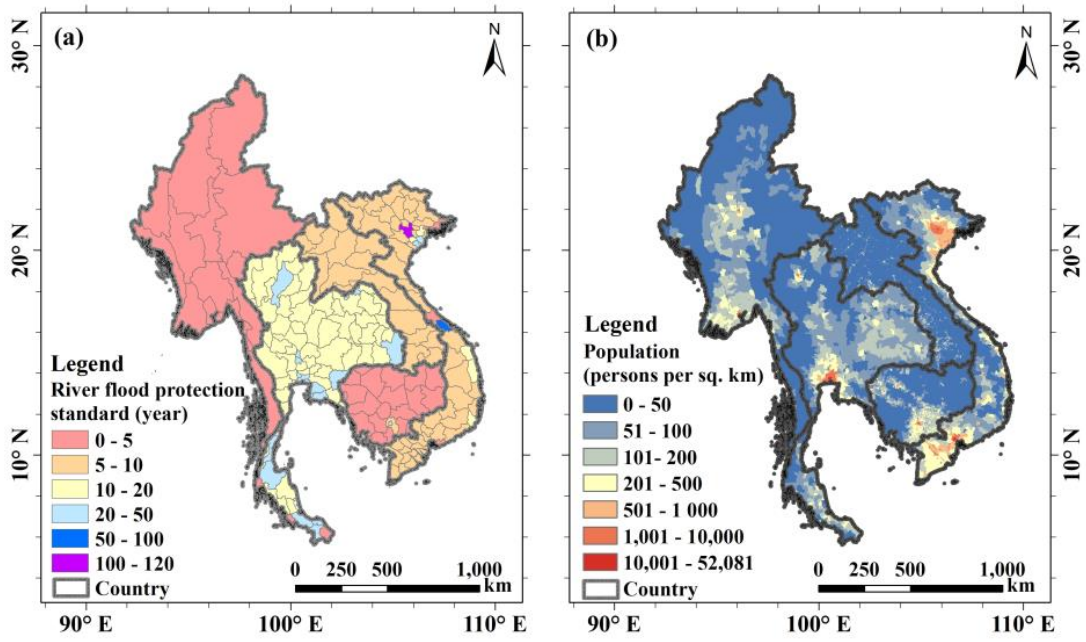

Figure 12. Spatial pattern of flood protection standards and population count in the Mainland Southeast Asia. (a) flood protection standards (year), and (b) gridded population in 2015 (persons per km^2). The flood protection standards data is FLOodPROtection Standards (FLOPROS) from Scussolini et al. (2016). Population data is Gridded Population of the World, Version 4 (GPWv4): Population Count, Revision 11 (CIESIN, 2018) (Figure 8 in paper III).

4.4 Future Change in Tropical Cyclone Intensity

In paper IV, comparison of best track and historical synthetics for 1981 – 2000 indicates that the downscaling technique is able to simulate synthetic storm events with compatible statistics of the best track's (Figure 13). Such reliabilities in simulating synthetic storm events in other regions have also been proven in previous studies (Emanuel 2017b; Kowch and Emanuel 2015; Zhu et al. 2013).

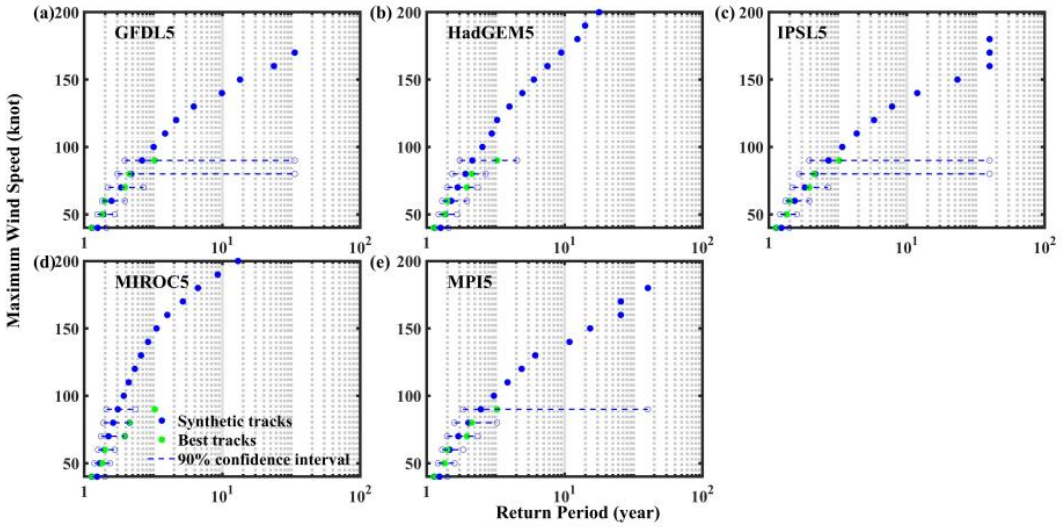

Figure 13. Comparison of return periods (unit: year) of the maximum wind speeds induced by tropical cyclones in the Mekong River Basin for 1981 – 2000 based on best track data and historical simulations from each of the five global climate models (GCMs): GFDL5 (a), HadGEM5 (b), IPSL5 (c), MIROC5 (d), and MPI5 (e). The green dots are for the best track data, and the blue dots are for five GCMs. The blue dashed lines show the 90% confidence interval based on estimated best track data sampling error (Figure 1 in paper IV).

Compared with 1981 – 2000, simulations present general shorter return periods of TC's MWS in the MRB in 2081 – 2100 under the RCP8.5 scenario based on the five GCMs, indicating increasing MWS of TCs influencing the MRB in the future (Figure 14). For instance, TC events with MWS of 140 knots that occur once every 98.7 years (median rate) at present, is predicted to occur once every 44.7 years in 2081 – 2100. This result discloses that the future TC intensity will be intensified in the MRB. The projected TC intensity increase is associated with increasing potential intensity under climate warming (Emanuel 2008, 2013). Specifically, climate warming will result in an increasing enthalpy jump at the sea surface. As the surface enthalpy fluxes is a decisive factor for TCs, such increase will facilitate the creation and development of TCs with higher intensity (Emanuel 2013; Emanuel and Sobel 2013). In

addition, climate warming associated smaller vertical wind shears may be another reason for the increases in TC intensity in Western North Pacific (Zhang et al. 2017a).

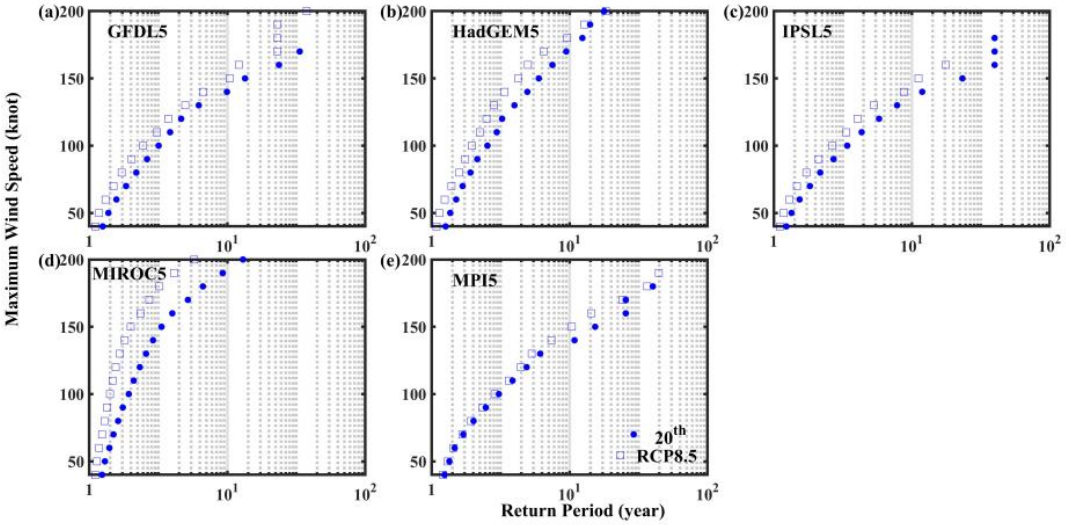

Figure 14. Return periods of the maximum wind speeds in the Mekong River Basin associated with synthetic tropical cyclones simulated from each of the five models over the period 1981 – 2000 from historical simulation (solid dots), and 2081 – 2100 from the RCP8.5 scenarios (hollow squares): GFDL5 (a), HadGEM5 (b), IPSL5 (c), MIROC5 (d), and MPI5 (e) (Figure 2 in paper IV).

Further analyses of the TC intensity in four selected major cities in the MRB (Can Tho, Phnom Penh, Nakhon Ratchasima, and Vientiane) show increasing TC intensity from high to low latitude at both periods (1981 – 2000 and 2081 – 2100) (Figure 3 in paper IV). On the one hand, consistent increasing TC intensities for 2081 – 2100 are estimated at Can Tho and Phnom Penh which are closer to the coast than the other two cities. On the other hand, the relatively smaller increases in TC intensity in the higher latitude area may result in substantial risk, because of the lacking experience in facing intense TCs in this area.

Fast coastal development, such as shipping, coastal tourism, and coastal settlement, has promoted more densely populated coastal areas than ever before (Merkens et al. 2016; Neumann et al. 2015), which drives higher exposure of assets to TC induced hazards. For example, increasing future TC intensity in a coastal area like Can Tho can have catastrophic damages. Also, intensified TCs are prone to induce storm surges in the coastal area (Lin et al. 2012; Powell and Reinhold 2007), which will be further amplified by the future rising sea levels (Lin et al. 2016; Walsh et al. 2016) and sinking Mekong Delta (Erban et al. 2014). On top of increasing exposure, rising future TC

intensity will most likely escalate future TC associated wind and flood risks, particularly in these coastal areas (Woodruff et al. 2013).

Overall, TCs have extensive impacts on the MRB due to the associated extreme wind, rainfall, and floods. TC induced floods have caused high impacts on mortality and displacement rates. In the MRB countries, the poor inhabitants suffered the most from TCs and floods (ASEAN 2017; MRC 2010b; Hallegatte et al. 2017). Thailand and Vietnam are the two world's most important rice exporting countries (USDA 2019). The projected intensified TCs in the MRB could disturb rice production in these countries, particularly in the Mekong Delta, by means of heavy rainfall and storm surges, which may cause global food market disorder. Consequently, TCs have substantial impacts on the MRB and may imperil sustainable development, which could aggravate conflicts in the region and beyond.

5 Conclusions

The thesis aims at estimating the TC associated extreme wind, rainfall, and floods impact on the MRB, because of TCs' potential disastrous impacts. In general, this thesis evaluates the reliability of existing gridded precipitation datasets, estimates the changes in and impacts of TC associated rainfall and floods, and projects the future change in TC intensity in the MRB. Results show that TCs influence the MRB primarily by carrying extreme precipitation and causing floods. TC induced floods have substantial impacts on human mortality and displacement rates. The projected consistent increasing intensity of future TCs raises a concern about future rising TC related risks. Taking the TC impact on the MRB as a case study, this thesis provides advanced knowledge and understanding of the change in TCs and their impacts on the MRB and other areas facing similar issues. The scientific contributions of this thesis can be summarized as follows:

I. TRMM 3B42 and PERSIANN-CDR precipitation data show higher reliability on both spatial and temporal scales in the MRB than the reanalysis products (paper I).
II. TC induced rainfall plays a minor role in the annual mean total precipitation in the MRB, but TCs are crucial to the occurrence of extreme rainfall events, particularly at the eastern lower basin (paper II).
III. TC induced floods amount to 24.6% occurrence of all the occurred floods between 1985 and 2018; and TC induced floods cause relatively higher human mortality and displacement rates than the average of what all floods causes do (paper III).
IV. Compared with 1981 – 2000, shorter return periods of TC intensity in the MRB for 2081 – 2100 are projected based on five GCMs under the RCP8.5 scenario, indicating increases in the future TC associated risk (paper IV).

6 Future Research Outlook

To better understand how TCs influence the MRB, the thesis advances the understanding of the impact TC associated rainfall, and floods had in the past, as well as how the future TC intensity may change. Many more fundamental aspects of the hydroclimate, and socioeconomic impacts require research. For example, since the TC rainfall area varies along with the TC size, using techniques to outline TC rainfall swaths instead of a fixed TC radius, would provide more accurate TCR detection (Lin et al. 2015; Rios Gaona et al. 2018). Such analysis would offer a better understanding of the TCs contribution to producing extreme rainfall events in the MRB. Research has found intensified TC associated rainfall rates in other regions of the world, as a result of anthropogenic warming (Emanuel 2017a; Knutson et al. 2019; Risser and Wehner 2017). Have TC associated rainfall rates changed in the past in the MRB? The seasonal TC induced extreme rainfall pattern also requires research, which has not been investigated in this region. Moreover, how will this pattern change under the weakening Indian Summer Monsoon and East Asian Monsoon (Liu et al. 2019; Swapna et al. 2017)? All these questions aim to advance the understanding of TC associated extreme rainfall events.

Antecedent soil moisture is a critical factor linked to floods (Bennett et al. 2018; Do et al. 2020). TCs making landfall in the late monsoon season are prone to induce floods, partly because of the highly saturated anecdote soil caused by the monsoon rainfall (Delgado et al. 2010; MRC 2010a). More efforts should be done to explore how much the antecedent soil moisture induced by monsoon rainfall attribute to the floods induced by TCs. What is the difference between TCs making landfall in the pre-monsoon and post-monsoon seasons? Advanced understanding of these issues would benefit the estimation of TC induced floods and the associated socioeconomic impacts.

In addition, various projections indicate rising probability of intensified TCs under the future climate warming (Choi et al. 2019; Emanuel 2013; Walsh et al. 2016). In particular, there is medium-to-high confidence that TC intensity and the proportion of intense TCs will increase, as well as the TC rainfall rates under the 2 °C anthropogenic warming (Knutson et al. 2019). How the future TC rainfall rates and associated floods occurrences will change under climate warming in the MRB needs further research.

Ultimately, socioeconomic development is related to the impacts of TCs (Mendelsohn et al. 2012). Increasing wealth ("exposure") in the TC landfalling regions are the primary reason for the increasing TC related damages around the world during the past decades (Bouwer 2011; Pielke et al. 2008; Weinkle et al. 2012). Climate extremes' impact on economic losses and fatality have large spatial and interannual variabilities with higher economic loss in developed countries, and live loss rates in developing countries (IPCC 2012). In addition, combining the scenarios of projected socioeconomic global changes (Shared Socioeconomic Pathways [SSPs]), projections show coastward-migration under all the SSPs with the continuous future growth of coastal population (Merkens et al. 2016; Neumann et al. 2015), as well as a growing economy (Leimbach et al. 2017). More efforts are needed to estimate the future TC impact on societal development in the MRB, which shall consider the spatiotemporal changes of "exposure" and "vulnerability" (Woodruff et al. 2013).

References

ADB, 2009: *The Economics of Climate Change in Southeast Asia: A Regional* Review. Manila, Philippines: Asian Development Bank (ADB). 255 pp.

ASEAN, 2017: *ASEAN Statistical Report on Millennium Development Goals 2017.* Jakarta: The Association of Southeast Asian Nations (ASEAN).148 pp. www.asean.org.

Ashouri, H., K. L. Hsu, S. Sorooshian, D. K. Braithwaite, K. R. Knapp, L. D. Cecil, B. R. Nelson, and O. P. Prat, 2015: PERSIANN-CDR: Daily precipitation climate data record from multisatellite observations for hydrological and climate studies. *Bull. Am. Meteorol. Soc.*, **96**, 69–83, https://doi.org/10.1175/BAMS-D-13-00068.1.

Balica, S., Q. Dinh, I. Popescu, T. Q. Vo, and D. Q. Pham, 2014: Flood impact in the Mekong Delta, Vietnam. *J. Maps*, **10**, 257–268, https://doi.org/10.1080/17445647.2013.859636.

Balk, D. L., U. Deichmann, G. Yetman, F. Pozzi, S. I. Hay, and A. Nelson, 2006: Determining Global Population Distribution: Methods, Applications and Data. *Adv. Parasitol.*, **62**, 119–156, https://doi.org/10.1016/S0065-308X(05)62004-0.Determining.

Bangalore, M., A. Smith, and T. Veldkamp, 2019: Exposure to Floods, Climate Change, and Poverty in Vietnam. *Econ. Disasters Clim. Chang.*, 79–99, https://doi.org/https://doi.org/10.1007/s41885-018-0035-4.

Bengtsson, L., 2010: The global atmospheric water cycle. *Environ. Res. Lett.*, **5**, https://doi.org/10.1088/1748-9326/5/2/025202.

Bennett, B., M. Leonard, Y. Deng, and S. Westra, 2018: An empirical investigation into the effect of antecedent precipitation on flood volume. *J. Hydrol.*, **567**, 435–445, https://doi.org/10.1016/j.jhydrol.2018.10.025.

Betts, A. K., M. Zhao, P. A. Dirmeyer, and A. C. M. Beljaars, 2006: Comparison of ERA40 and NCEP/DOE near-surface data sets with other ISLSCP-II data sets. *J. Geophys. Res. Atmos.*, **111**, 1–20, https://doi.org/10.1029/2006JD007174.

Bouwer, L. M., 2011: Have disaster losses increased due to anthropogenic climate change? *Bull. Am. Meteorol. Soc.*, **92**, 39–46, https://doi.org/10.1175/2010BAMS3092.1.

Brakenridge, G. R., 2019: Global Active Archive of Large Flood Events. *Dartmouth Flood Obs. Univ. Color.*,. http://floodobservatory.colorado.edu/Archives/index.html (Accessed May 15, 2019).

Camargo, S. J., 2013: Global and Regional Aspects of Tropical Cyclone Activity in the CMIP5 Models. *J. Clim.*, **26**, 9880–9902, https://doi.org/10.1175/JCLI-D-12-00549.1.

Camargo, S. J., and A. H. Sobel, 2005: Western North Pacific tropical cyclone intensity and ENSO. *J. Clim.*, **18**, 2996–3006, https://doi.org/10.1175/JCLI3457.1.

Camargo, S. J., M. C. Wheeler, and A. H. Sobel, 2009: Diagnosis of the MJO modulation of tropical cyclogenesis using an empirical index. *J. Atmos. Sci.*, **66**, 3061–3074, https://doi.org/10.1175/2009JAS3101.1.

Camargo, S. J., A. H. Sobel, A. G. Barnston, and P. J. Klotzbach, 2010: The influence of natural climate variability on tropical cyclones and seasonal forecasts of tropical cyclone activity. *Glob. Perspect. Trop. Cyclones, from Sci. to Mitig.*, 325–360.

Chau, V. N., J. Holland, S. Cassells, and M. Tuohy, 2013: Using GIS to map impacts upon agriculture from extreme floods in Vietnam. *Appl. Geogr.*, **41**, 65–74, https://doi.org/10.1016/j.apgeog.2013.03.014.

Chen, J. M., H. S. Chen, and J. S. Liu, 2013a: Coherent interdecadal variability of tropical cyclone rainfall and seasonal rainfall in taiwan during october. *J. Clim.*, **26**, 308–321, https://doi.org/10.1175/JCLI-D-11-00697.1.

Chen, Y., E. E. Ebert, K. J. E. Walsh, and N. E. Davidson, 2013b: Evaluation of TRMM 3B42 precipitation estimates of tropical cyclone rainfall using PACRAIN data. *J. Geophys. Res. Atmos.*, **118**, 2184–2196, https://doi.org/10.1002/jgrd.50250.

Chhin, R., N. J. Trilaksono, and T. W. Hadi, 2016: Tropical cyclone rainfall structure affecting indochina peninsula and lower mekong river basin (LMB). *J. Phys. Conf. Ser.*, **739**, https://doi.org/10.1088/1742-6596/739/1/012103.

Choi, W., C. H. Ho, J. Kim, and J. C. L. Chan, 2019: Near-future tropical cyclone predictions in the western North Pacific: fewer tropical storms but more typhoons. *Clim. Dyn.*, **53**, 1341–1356, https://doi.org/10.1007/s00382-019-04647-x.

CIESIN, 2011: *Foresight Project on Migration and Global Environmental Change, Report MR4: Estimating Net Migration by Ecosystem and by Decade,1970-2010*. The Center for International Earth Science Information Network (CIESIN).

CIESIN, 2017: Global Population Count Grid Time Series Estimates. The Center for International Earth Science Information Network (CIESIN). *Palisades, NY NASA Socioecon. Data Appl. Cent.*,. the Center for International Earth Science Information Network (CIESIN), https://doi.org/10.7927/H4CC0XNV (Accessed May 15, 2019).

CIESIN, 2018: Gridded Population of the World, Version 4 (GPWv4): Population Count, Revision 11. The Center for International Earth Science Information Network (CIESIN). *Palisades, NY NASA Socioecon. Data Appl. Cent.*, https://doi.org/10.7927/H4JW8BX5. (Accessed May 15, 2019).

Collins, W. J., and Coauthors, 2011: Development and evaluation of an Earth-System model – HadGEM2. *Geosci. Model Dev.*, **4**, 1051–1075, https://doi.org/10.5194/gmd-4-1051-2011.

CRED, 2019: *EM-DAT: The International Disaster Database, Centre for Research on the Epidemiology of Disasters (CRED). Accessed on 17 June 2019. [Available online at www.emdat.be/]*. accessed 17 June 2019 pp. www.emdat.be/.

Cunado, J., and S. Ferreira, 2015: The Macroeconomic Impacts of Natural Disasters: The Case of Floods. *Land Econ.*, **90**, 149–168, https://doi.org/10.3368/le.90.1.149.

Darby, S. E., J. Leyland, M. Kummu, T. A. Räsänen, and H. Lauri, 2013: Decoding the drivers of bank erosion on the Mekong river: The roles of the Asian monsoon, tropical storms, and snowmelt. *Water Resour. Res.*, **49**, 2146–2163, https://doi.org/10.1002/wrcr.20205.

Darby, S. E., and Coauthors, 2016: Fluvial sediment supply to a mega-delta reduced by shifting tropical-cyclone activity. *Nature*, **539**, 276–279, https://doi.org/10.1038/nature19809.

Decker, M., M. A. Brunke, Z. Wang, K. Sakaguchi, X. Zeng, and M. G. Bosilovich, 2012: Evaluation of the reanalysis products from GSFC, NCEP, and ECMWF using flux tower observations. *J. Clim.*, **25**, 1916–1944, https://doi.org/10.1175/JCLI-D-11-00004.1.

Dee, D. P., and Coauthors, 2011: The ERA-Interim reanalysis: Configuration and performance of the data assimilation system. *Q. J. R. Meteorol. Soc.*, **137**, 553–597, https://doi.org/10.1002/qj.828.

Delgado, J. M., B. Merz, and H. Apel, 2010: Flood trends and variability in the Mekong river. *Assembly*, **14**, 407–418.

Delgado, J. M., B. Merz, and H. Apel, 2012: A climate-flood link for the lower Mekong River. *Hydrol. Earth Syst. Sci.*, **16**, 1533–1541, https://doi.org/10.5194/hess-16-1533-2012.

Diamond, H. J., A. M. Lorrey, and J. A. Renwick, 2013: A southwest pacific tropical cyclone climatology and linkages to the El Ni??o-Southern Oscillation. *J. Clim.*, **26**, 3–25, https://doi.org/10.1175/JCLI-D-12-00077.1.

Do, H. X., S. Westra, M. Leonard, and L. Gudmundsson, 2020: Global-Scale Prediction of Flood Timing Using Atmospheric Reanalysis. *Water Resour. Res.*, **56**, 1–19, https://doi.org/10.1029/2019WR024945.

Donat, M. G., and Coauthors, 2013: Updated analyses of temperature and precipitation extreme indices since the beginning of the twentieth century: The HadEX2 dataset. *J. Geophys. Res. Atmos.*, **118**, 2098–2118, https://doi.org/10.1002/jgrd.50150.

Donner, L. J., and Coauthors, 2011: The dynamical core, physical parameterizations, and basic simulation characteristics of the

atmospheric component AM3 of the GFDL global coupled model CM3. *J. Clim.*, **24**, 3484–3519, https://doi.org/10.1175/2011JCLI3955.1.

Doocy, S., A. Dick, A. Daniels, and T. D. Kirsch, 2013: The Human Impact of Tropical Cyclones: A Historical Review. *PLoS Curr. Disasters*, 1–38, https://doi.org/10.1371/currents.dis.2664354a5571512063ed29d25ffbce74.Authors.

Doxsey-Whitfield, E., K. MacManus, S. B. Adamo, L. Pistolesi, J. Squires, O. Borkovska, and S. R. Baptista, 2015: Taking Advantage of the Improved Availability of Census Data: A First Look at the Gridded Population of the World, Version 4. *Pap. Appl. Geogr.*, **1**, 226–234, https://doi.org/10.1080/23754931.2015.1014272.

Dufresne, J. L., and Coauthors, 2013: *Climate change projections using the IPSL-CM5 Earth System Model: From CMIP3 to CMIP5*. 2123–2165 pp.

Eastham, J., F. Mpelasoka, C. Ticehurst, P. Dyce, R. Ali, and M. Kirby, 2008: *Mekong River Basin Water Resources Assessment: Impacts of Climate Change*. 153 pp.

Elsner, J. B., and K. B. Liu, 2003: Examining the ENSO-typhoon hypothesis. *Clim. Res.*, **25**, 43–54, https://doi.org/10.3354/cr025043.

Emanuel, K., 2006: Climate and tropical cyclone activity: A new model downscaling approach. *J. Clim.*, **19**, 4797–4802, https://doi.org/10.1175/JCLI3908.1.

Emanuel, K., 2008: The hurricane-climate connection. *Bull. Am. Meteorol. Soc.*, **89**, ES10–ES20, https://doi.org/10.1175/BAMS-89-5-Emanuel.

Emanuel, K., 2013: Downscaling CMIP5 climate models shows increased tropical cyclone activity over the 21st century. *Proc. Natl. Acad. Sci.*, **110**, 12219–12224, https://doi.org/10.1073/pnas.1301293110.

Emanuel, K., 2017a: Assessing the present and future probability of Hurricane Harvey's rainfall. *Proc. Natl. Acad. Sci.*, **0**, 201716222, https://doi.org/10.1073/pnas.1716222114.

Emanuel, K., 2017b: Will global warming make hurricane forecasting more difficult? *Bull. Am. Meteorol. Soc.*, **98**, 495–501, https://doi.org/10.1175/BAMS-D-16-0134.1.

Emanuel, K., and A. Sobel, 2013: Response of tropical sea surface temperature, precipitation, and tropical cyclone-related variables to changes in global and local forcing. *J. Adv. Model. Earth Syst.*, **5**, 447–458, https://doi.org/10.1002/jame.20032.

Emanuel, K., S. Ravela, E. Vivant, and C. Risi, 2006: A statistical deterministic approach to hurricane risk assessment. *Bull. Am. Meteorol. Soc.*, **87**, 299–314, https://doi.org/10.1175/BAMS-87-3-299.

Emanuel, K., R. Sundararajan, and J. Williams, 2008: Hurricanes and global warming: Results from downscaling IPCC AR4 simulations. *Bull. Am. Meteorol. Soc.*, **89**, 347–367, https://doi.org/10.1175/BAMS-89-3-347.

Erban, L. E., S. M. Gorelick, and H. A. Zebker, 2014: Groundwater extraction, land subsidence, and sea-level rise in the Mekong Delta, Vietnam. *Environ. Res. Lett.*, **9**, https://doi.org/10.1088/1748-9326/9/8/084010.

Feng, L., and T. Zhou, 2012: Water vapor transport for summer precipitation over the Tibetan Plateau: Multidata set analysis. *J. Geophys. Res. Atmos.*, **117**, 1–16, https://doi.org/10.1029/2011JD017012.

Frank, W. M., 1977: The structure and energetics of the tropical cyclone I. strom structure. *Mon. Weather Rev.*, **105**, 1119–1135.

Fu, G., Z. Liu, S. P. Charles, Z. Xu, and Z. Yao, 2013: A score-based method for assessing the performance of GCMs: A case study of southeastern Australia. *J. Geophys. Res. Atmos.*, **118**, 4154–4167, https://doi.org/10.1002/jgrd.50269.

Gale, E. L., and M. A. Saunders, 2013: The 2011 Thailand flood: climate causes and return periods. *Weather*, **68**, 233–237, https://doi.org/10.1002/wea.2133.

Gelaro, R., and Coauthors, 2017: The modern-era retrospective analysis for research and applications, version 2 (MERRA-2). *J. Clim.*, **30**, 5419–5454, https://doi.org/10.1175/JCLI-D-16-0758.1.

Giorgetta, M. A., and Coauthors, 2013: Climate and carbon cycle changes from 1850 to 2100 in MPI-ESM simulations for the Coupled Model Intercomparison Project phase 5. *J. Adv. Model. Earth Syst.*, **5**, 572–597, https://doi.org/10.1002/jame.20038.

Goh, A. Z. C., and J. C. L. Chan, 2010: Interannual and interdecadal variations of tropical cyclone activity in the South China Sea. *Int. J. Climatol.*, **30**, 827–843, https://doi.org/10.1002/joc.1943.

Gray, W. M., 1968: Global View of the Origin of Tropical Disturbances and Storms. *Mon. Weather Rev.*, **96**, 669–700, https://doi.org/10.1175/1520-0493(1968)096<0669:gvotoo>2.0.co;2.

Ha, K.-J., B.-H. Kim, E.-S. Chung, J. C. L. Chan, and C.-P. Chang, 2020: Major factors of global and regional monsoon rainfall changes: natural versus anthropogenic forcing. *Environ. Res. Lett.*, **15**, 034055, https://doi.org/10.1088/1748-9326/ab7767.

Hallegatte, S., A. Vogt-Schilb, M. Bangalore, and J. Rozenberg, 2017: *Unbreakable: Building the Resilience of the Poor in the Face of Natural Disasters. Climate Change and Development Series.* 201pp pp.

Haraguchi, M., and U. Lall, 2015: Flood risks and impacts: A case study of Thailand's floods in 2011 and research questions for supply chain decision making. *Int. J. Disaster Risk Reduct.*, **14**, 256–272, https://doi.org/10.1016/j.ijdrr.2014.09.005.

Henderson-Sellers, A., and Coauthors, 1998: Tropical Cyclones and Global Climate Change: A Post-IPCC Assessment. *Bull. Am. Meteorol. Soc.*, **79**, 19–38, https://doi.org/10.1175/1520-

0477(1998)079<0019:tcagcc>2.0.co;2.

Hoang, L. P., and Coauthors, 2016: Mekong River flow and hydrological extremes under climate change. *Hydrol. Earth Syst. Sci.*, **20**, 3027–3041, https://doi.org/10.5194/hess-20-3027-2016.

Holmes, J. A., E. R. Cook, and B. Yang, 2009: Climate change over the past 2000 years in Western China. *Quat. Int.*, **194**, 91–107, https://doi.org/10.1016/j.quaint.2007.10.013.

Hu, P., Q. Zhang, P. Shi, B. Chen, and J. Fang, 2018: Flood-induced mortality across the globe: Spatiotemporal pattern and influencing factors. *Sci. Total Environ.*, **643**, 171–182, https://doi.org/10.1016/j.scitotenv.2018.06.197.

Huang, A., Y. Zhao, Y. Zhou, B. Yang, L. Zhang, X. Dong, D. Fang, and Y. Wu, 2016: Evaluation of multisatellite precipitation products by use of ground-based data over China. *J. Geophys. Res. Atmos.*, 10654–10675, https://doi.org/10.1002/ 2016JD025456.

Huffman, G. J., and D. T. Bolvin, 2012: TRMM and other data precipita- tion data set documentation (ftp://meso-a.gsfc.nasa.gov/pub/trmmdocs/ 3B42_3B43_doc.pdf). 1–3.

Huffman, G. J., and Coauthors, 2007: The TRMM Multisatellite Precipitation Analysis (TMPA): Quasi-Global, Multiyear, Combined-Sensor Precipitation Estimates at Fine Scales. *J. Hydrometeorol.*, **8**, 38–55, https://doi.org/10.1175/JHM560.1.

Imbach, P., and Coauthors, 2018: Future climate change scenarios in Central America at high spatial resolution. *PLoS One*, **13**, 1–21, https://doi.org/10.1371/journal.pone.0193570.

IPCC, 2012: *Managing the Risks of Extreme Events and Disasters to Advance Climate Change Adaptation*. The Intergovernmental Panel on Climate Change (IPCC). 582 pp. https://www.ipcc.ch/report/managing-the-risks-of-extreme-events-and-disasters-to-advance-climate-change-adaptation/.

IPCC, 2013: Climate Change 2013: The Physical Science Basis. *Contribution of Working Group I to the Fifth Assessment Report of the Intergovernmental Panel on Climate Change*, V.B. and P.M.M. Stocker, T.F., D. Qin, G.-K. Plattner, M. Tignor, S.K. Allen, J. Boschung, A. Nauels, Y. Xia, Ed., Cambridge University Press, 1535 pp.

Jiang, H., and E. J. Zipser, 2010: Contribution of Tropical Cyclones to the Global Precipitation from Eight Seasons of TRMM Data: Regional, Seasonal, and Interannual Variations. *J. Clim.*, **23**, 1526–1543, https://doi.org/10.1175/2009JCLI3303.1.

Jongman, B., and Coauthors, 2014: Increasing stress on disaster-risk finance due to large floods. *Nat. Clim. Chang.*, **4**, 264–268, https://doi.org/10.1038/nclimate2124.

Jonkman, S. N., 2005: Global Perspectives on Loss of Human Life Caused by Floods. *Nat. Hazards*, **34**, 151–175, https://doi.org/https://doi.org/10.1007/s11069-004-8891-3.

Jonkman, S. N., B. Maaskant, E. Boyd, and M. L. Levitan, 2009: Loss of life caused by the flooding of New Orleans after hurricane Katrina: Analysis of the relationship between flood characteristics and mortality. *Risk Anal.*, **29**, 676–698, https://doi.org/10.1111/j.1539-6924.2008.01190.x.

Kendall, M. G., 1938: A New Measure of Rank Correlation. *Biometrika*, **30**, 81, https://doi.org/10.2307/2332226.

Keskinen, M., 2008: Water resources development and impact assessment in the Mekong Basin: Which way to go? *Ambio*, **37**, 193–198, https://doi.org/10.1579/0044-7447(2008)37[193:WRDAIA]2.0.CO;2.

Khouakhi, A., G. Villarini, and G. A. Vecchi, 2017: Contribution of tropical cyclones to rainfall at the global scale. *J. Clim.*, **30**, 359–372, https://doi.org/10.1175/JCLI-D-16-0298.1.

Knapp, K. R., M. C. Kruk, D. H. Levinson, H. J. Diamond, and C. J. Neumann, 2010: The International Best Track Archive for Climate Stewardship (Ibtracs) Unifying Tropical Cyclone Data. *Bull. Am. Meteorol. Soc.*, **91**, 362-+, https://doi.org/10.1175/2009BAMS2755.1.

Knutson, T., and Coauthors, 2019: Tropical Cyclones and Climate Change Assessment: Part II. Projected Response to Anthropogenic Warming. *Bull. Am. Meteorol. Soc.*, 1–62, https://doi.org/10.1175/bams-d-18-0194.1.

Knutson, T. R., J. J. Sirutis, M. Zhao, R. E. Tuleya, M. Bender, G. A. Vecchi, G. Villarini, and D. Chavas, 2015: Global projections of intense tropical cyclone activity for the late twenty-first century from dynamical downscaling of CMIP5/RCP4.5 scenarios. *J. Clim.*, **28**, 7203–7224, https://doi.org/10.1175/JCLI-D-15-0129.1.

Kowch, R., and K. Emanuel, 2015: Are Special Processes at Work in the Rapid Intensification of Tropical Cyclones? *Mon. Weather Rev.*, **143**, 878–882, https://doi.org/10.1175/MWR-D-14-00360.1.

Lauri, H., T. A. Räsänen, and M. Kummu, 2014: Using Reanalysis and Remotely Sensed Temperature and Precipitation Data for Hydrological Modeling in Monsoon Climate: Mekong River Case Study. *J. Hydrometeorol.*, **15**, 1532–1545, https://doi.org/10.1175/JHM-D-13-084.1.

Lee, T. C., C. Y. Y. Leung, M. H. Kok, and H. S. Chan, 2012: The long term variations of tropical cyclone activity in the South China Sea and the vicinity of Hong Kong. *Trop. Cyclone Res. Rev.*, **1**, 277–292, https://doi.org/10.6057/2012TCRR02.01.

Leimbach, M., E. Kriegler, N. Roming, and J. Schwanitz, 2017: Future growth patterns of world regions – A GDP scenario approach. *Glob. Environ.*

Chang., **42**, 215–225, https://doi.org/10.1016/j.gloenvcha.2015.02.005.

Lestari, S., J.-I. Hamada, F. Syamsudin, Sunaryo, J. Matsumoto, and M. D. Yamanaka, 2016: ENSO Influences on Rainfall Extremes around Sulawesi and Maluku Islands in the Eastern Indonesian Maritime Continent. *Sola*, **12**, 37–41, https://doi.org/10.2151/sola.2016-008.

Lin, N., K. Emanuel, M. Oppenheimer, and E. Vanmarcke, 2012: Physically based assessment of hurricane surge threat under climate change. *Nat. Clim. Chang.*, **2**, 462–467, https://doi.org/10.1038/nclimate1389.

Lin, N., R. E. Kopp, B. P. Horton, and J. P. Donnelly, 2016: Hurricane Sandy's flood frequency increasing from year 1800 to 2100. *Proc. Natl. Acad. Sci.*, **113**, 12071–12075, https://doi.org/10.1073/pnas.1604386113.

Lin, Y., M. Zhao, and M. Zhang, 2015: Tropical cyclone rainfall area controlled by relative sea surface temperature. *Nat. Commun.*, **6**, 1–7, https://doi.org/10.1038/ncomms7591.

Liu, K. S., and J. C. L. Chan, 2013: Inactive period of Western North Pacific tropical cyclone activity in 1998-2011. *J. Clim.*, **26**, 2614–2630, https://doi.org/10.1175/JCLI-D-12-00053.1.

Liu, Y., and Coauthors, 2019: Anthropogenic Aerosols Cause Recent Pronounced Weakening of Asian Summer Monsoon Relative to Last Four Centuries. *Geophys. Res. Lett.*, **46**, 5469–5479, https://doi.org/10.1029/2019GL082497.

Lutz, A., W. Terink, P. Droogers, W. Immerzeel, and T. Piman, 2014: *Development of baseline climate data set and trend analysis in the Mekong Basin*. 1–127 pp. http://www.futurewater.nl.

Martin, U., 2015: Health after disaster: A perspective of psychological/health reactions to disaster. *Cogent Psychol.*, **2**, https://doi.org/10.1080/23311908.2015.1053741.

Mendelsohn, R., K. Emanuel, S. Chonabayashi, and L. Bakkensen, 2012: The impact of climate change on global tropical cyclone damage. *Nat. Clim. Chang.*, **2**, 205–209, https://doi.org/10.1038/nclimate1357.

Merkens, J., L. Reimann, J. Hinkel, and A. T. Vafeidis, 2016: Gridded population projections for the coastal zone under the Shared Socioeconomic Pathways. *Glob. Planet. Change*, **145**, 57–66, https://doi.org/10.1016/j.gloplacha.2016.08.009.

Molinari, J., and D. Vollaro, 2013: What percentage of western north pacific tropical cyclones form within the monsoon trough? *Mon. Weather Rev.*, **141**, 499–505, https://doi.org/10.1175/MWR-D-12-00165.1.

Moriasi, D. N., J. G. Arnold, M. W. Van Liew, R. L. Bingner, R. D. Harmel, and T. L. Veith, 2007: Model Evaluation Guidelines for Systematic Quantification of Accuracy in Watershed Simulations. *Trans. ASABE*, **50**, 885–900.

MRC, 2005: Overview of the Hydrology of the Mekong Basin. Vientiane, Laos: *Mekong River Commission*. 73 pp, https://doi.org/1728 3248.

MRC, 2007: *Annual Mekong Flood Report 2006.* Vientiane, Laos: *Mekong River Commission*. 76 pp. www.mrcmekong.org.

MRC, 2010a: *State of the Basin Report 2010.* Vientiane, Laos: *Mekong River Commission*. 232 pp. www.mrcmekong.org.

MRC, 2010b: *Annual Mekong Flood Report 2009.* Vientiane, Laos: *Mekong River Commission*. 95 pp. www.mrcmekong.org.

MRC, 2011: *Agriculture and Irrigation Programme : 2011-2015 Programme Document.* Vientiane, Laos: *Mekong River Commission*. 94 pp. www.mrcmekong.org.

MRC, 2014: *Annual Mekong Flood Report 2011.* Vientiane, Laos: *Mekong River Commission*. 72 pp. www.mrcmekong.org.

MRC, 2015: *Annual Mekong Flood Report 2013.* Vientiane, Laos: *Mekong River Commission*. 89 pp. www.mrcmekong.org.

Nash, J. E., and J. V Sutcliffe, 1970: River Flow Forecasting Through Conceptual Models Part I-a Discussion of Principles*. *J. Hydrol.*, **10**, 282–290, https://doi.org/10.1016/0022-1694(70)90255-6.

Nasrollahi, N., K. Hsu, and S. Sorooshian, 2013: An Artificial Neural Network Model to Reduce False Alarms in Satellite Precipitation Products Using MODIS and CloudSat Observations. *J. Hydrometeorol.*, **14**, 1872–1883, https://doi.org/10.1175/JHM-D-12-0172.1.

Neumann, B., A. T. Vafeidis, J. Zimmermann, and R. J. Nicholls, 2015: Future Coastal Population Growth and Exposure to Sea-Level Rise and Coastal Flooding - A Global Assessment. https://doi.org/10.1371/journal.pone.0118571.

Neumayer, E., and F. Barthel, 2011: Normalizing economic loss from natural disasters: A global analysis. *Glob. Environ. Chang.*, **21**, 13–24, https://doi.org/10.1016/j.gloenvcha.2010.10.004.

Ng, E. K. W., and J. C. L. Chan, 2012: Interannual variations of tropical cyclone activity over the north Indian Ocean. *Int. J. Climatol.*, **32**, 819–830, https://doi.org/10.1002/joc.2304.

Nguyen-Thi, H. A., J. Matsumoto, T. Ngo-Duc, and N. Endo, 2012a: A Climatological Study of Tropical Cyclone Rainfall in Vietnam. *Sola*, **8**, 41–44, https://doi.org/10.2151/sola.2012-011.

Nguyen-Thi, H. A., J. Matsumoto, N. Thanh, and N. Endo, 2012b: Long-term trends in tropical cyclone rainfall in Vietnam ISSN 1995-6983. *J. Agrofor. Environ.*, **6**, 89–92.

Nguyen, H. N., 2008: *Human Development Report 2007 / 2008 Flooding in Mekong River Delta , Viet Nam*. 4 pp.

Palmer, L., 2013: Providing aid before climate disasters strike. *Nat. Clim.*

Chang., **3**, 857–858, https://doi.org/10.1038/nclimate2016.

Park, D. S. R., C. H. Ho, J. H. Kim, and H. S. Kim, 2011: Strong landfall typhoons in Korea and Japan in a recent decade. *J. Geophys. Res. Atmos.*, **116**, 1–11, https://doi.org/10.1029/2010JD014801.

Park, D. S. R., C. H. Ho, and J. H. Kim, 2014: Growing threat of intense tropical cyclones to East Asia over the period 1977-2010. *Environ. Res. Lett.*, **9**, https://doi.org/10.1088/1748-9326/9/1/014008.

Payne, A. E., and Coauthors, 2020: Responses and impacts of atmospheric rivers to climate change. *Nat. Rev. Earth Environ.*, **1**, 143–157, https://doi.org/10.1038/s43017-020-0030-5.

Pech, S., and K. Sunada, 2008: Population growth and natural-resources pressures in the Mekong River Basin. *Ambio*, **37**, 219–224, https://doi.org/10.1579/0044-7447(2008)37[219:PGANPI]2.0.CO;2.

Peduzzi, P., B. Chatenoux, H. Dao, A. De Bono, C. Herold, J. Kossin, F. Mouton, and O. Nordbeck, 2012: Global trends in tropical cyclone risk. *Nat. Clim. Chang.*, **2**, 289–294, https://doi.org/10.1038/nclimate1410.

Pfahl, S., P. A. O'Gorman, and E. M. Fischer, 2017: Understanding the regional pattern of projected future changes in extreme precipitation. *Nat. Clim. Chang.*, **7**, 423–427, https://doi.org/10.1038/nclimate3287.

Pielke, J., A. Roger, J. Gratz, C. W. Landsea, D. Collins, M. A. Saunders, and R. Musulin, 2008: Normalized Hurricane Damage in the United States: 1900–2005. *Nat. Hazards Rev.*, **9**, 29–42, https://doi.org/10.1061/(ASCE)1527-6988(2008)9:1(29).

Powell, M. D., and T. A. Reinhold, 2007: Tropical Cyclone Destructive Potential by Integrated Kinetic Energy. *Bull. Am. Meteorol. Soc.*, **88**, 513–526, https://doi.org/10.1175/BAMS-88-4-513.

Rana, S., J. McGregor, and J. Renwick, 2015: Precipitation Seasonality over the Indian Subcontinent: An Evaluation of Gauge, Reanalyses, and Satellite Retrievals. *J. Hydrometeorol.*, **16**, 631–651, https://doi.org/10.1175/JHM-D-14-0106.1.

Rappaport, E. N., 2000: Loss of life in the United States associated with recent Atlantic tropical cyclones. *Bull. Am. Meteorol. Soc.*, **81**, 2065–2073, https://doi.org/10.1175/1520-0477(2000)081<2065:LOLITU>2.3.CO;2.

Rappaport, E. N., 2014: Fatalities in the united states from atlantic tropical cyclones: New data and interpretation. *Bull. Am. Meteorol. Soc.*, **95**, 341–346, https://doi.org/10.1175/BAMS-D-12-00074.1.

Räsänen, T. A., and M. Kummu, 2013: Spatiotemporal influences of ENSO on precipitation and flood pulse in the Mekong River Basin. *J. Hydrol.*, **476**, 154–168, https://doi.org/10.1016/j.jhydrol.2012.10.028.

Räsänen, T. A., V. Lindgren, J. H. A. Guillaume, B. M. Buckley, and M. Kummu, 2016: On the spatial and temporal variability of ENSO

precipitation and drought teleconnection in mainland Southeast Asia. *Clim. Past*, **12**, 1889–1905, https://doi.org/10.5194/cp-12-1889-2016.

Reichle, R. H., C. S. Draper, Q. Liu, M. Girotto, S. P. P. Mahanama, R. D. Koster, and G. J. M. De Lannoy, 2017a: Assessment of MERRA-2 land surface hydrology estimates. *J. Clim.*, **30**, 2937–2960, https://doi.org/10.1175/JCLI-D-16-0720.1.

Reichle, R. H., Q. Liu, R. D. Koster, C. S. Draper, S. P. P. Mahanama, and G. S. Partyka, 2017b: Land Surface Precipitation in MERRA-2. *J. Clim.*, **30**, 1643–1664, https://doi.org/10.1175/JCLI-D-16-0570.1.

Rios Gaona, M. F., G. Villarini, W. Zhang, and G. A. Vecchi, 2018: The added value of IMERG in characterizing rainfall in tropical cyclones. *Atmos. Res.*, **209**, 95–102, https://doi.org/10.1016/j.atmosres.2018.03.008.

Risser, M. D., and M. F. Wehner, 2017: Attributable Human-Induced Changes in the Likelihood and Magnitude of the Observed Extreme Precipitation during Hurricane Harvey. *Geophys. Res. Lett.*, **44**, 12,457-12,464, https://doi.org/10.1002/2017GL075888.

Saha, S., and Coauthors, 2010: The NCEP climate forecast system reanalysis. *Bull. Am. Meteorol. Soc.*, **91**, 1015–1057, https://doi.org/10.1175/2010BAMS3001.1.

Sahoo, B., and P. K. Bhaskaran, 2016: Assessment on historical cyclone tracks in the Bay of Bengal , east coast of India. *Int. J. Climatol.*, **109**, 95–109, https://doi.org/10.1002/joc.4331.

Schreck, C. J., J. Molinari, and A. Aiyyer, 2012: A global view of equatorial waves and tropical cyclogenesis. *Mon. Weather Rev.*, **140**, 774–788, https://doi.org/10.1175/MWR-D-11-00110.1.

Scussolini, P., J. C. J. H. Aerts, B. Jongman, L. M. Bouwer, H. C. Winsemius, H. De Moel, and P. J. Ward, 2016: FLOPROS: an evolving global database of flood protection standards. *Nat. Hazards Earth Syst. Sci.*, **16**, 1049–1061, https://doi.org/10.5194/nhess-16-1049-2016.

Sen, P. K., 1968: Estimates of the Regression Coefficient Based on Kendall's Tau. *J. Am. Stat. Assoc.*, **63**, 1379–1389, https://doi.org/10.1080/01621459.1968.10480934.

Seneviratne, S. I., D. Lüthi, M. Litschi, and C. Schär, 2006: Land-atmosphere coupling and climate change in Europe. *Nature*, **443**, 205–209, https://doi.org/10.1038/nature05095.

Seyyedi, H., E. N. Anagnostou, E. Beighley, and J. McCollum, 2015: Hydrologic evaluation of satellite and reanalysis precipitation datasets over a mid-latitude basin. *Atmos. Res.*, **164**–**165**, 37–48, https://doi.org/10.1016/j.atmosres.2015.03.019.

Sidike, A., X. Chen, T. Liu, K. Durdiev, and Y. Huang, 2016: Investigating alternative climate data sources for hydrological simulations in the

upstream of the Amu Darya river. *Water (Switzerland)*, **8**, https://doi.org/10.3390/w8100441.

Sohn, S. J., C. Y. Tam, K. Ashok, and J. B. Ahn, 2012: Quantifying the reliability of precipitation datasets for monitoring large-scale East Asian precipitation variations. *Int. J. Climatol.*, **32**, 1520–1526, https://doi.org/10.1002/joc.2380.

Sorooshian, S., K. L. Hsu, X. Gao, H. V. Gupta, B. Imam, and D. Braithwaite, 2000: Evaluation of PERSIANN system satellite-based estimates of tropical rainfall. *Bull. Am. Meteorol. Soc.*, **81**, 2035–2046, https://doi.org/10.1175/1520-0477(2000)081<2035:EOPSSE>2.3.CO;2.

Sun, Q., C. Miao, Q. Duan, H. Ashouri, S. Sorooshian, and K. L. Hsu, 2018: A Review of Global Precipitation Data Sets: Data Sources, Estimation, and Intercomparisons. *Rev. Geophys.*, **56**, 79–107, https://doi.org/10.1002/2017RG000574.

Swapna, P., J. Jyoti, R. Krishnan, N. Sandeep, and S. M. Griffies, 2017: Multidecadal Weakening of Indian Summer Monsoon Circulation Induces an Increasing Northern Indian Ocean Sea Level. *Geophys. Res. Lett.*, **44**, 10,560-10,572, https://doi.org/10.1002/2017GL074706.

Takahashi, H. G., and T. Yasunari, 2008: Decreasing Trend in Rainfall over Indochina during the Late Summer Monsoon : Impact of Tropical Cyclones. *J. Meteorol. Soc. Japan*, **86**, 429–438.

Takahashi, H. G., H. Fujinami, T. Yasunari, J. Matsumoto, and S. Baimoung, 2015: Role of tropical cyclones along the monsoon trough in the 2011 Thai flood and interannual variability. *J. Clim.*, **28**, 1465–1476, https://doi.org/10.1175/JCLI-D-14-00147.1.

Tan, M. L., P. W. Gassman, and A. P. Cracknell, 2017: Assessment of three long-term gridded climate products for hydro-climatic simulations in tropical river basins. *Water (Switzerland)*, **9**, https://doi.org/10.3390/w9030229.

Tanarhte, M., P. Hadjinicolaou, and J. Lelieveld, 2012: Intercomparison of temperature and precipitation data sets based on observations in the Mediterranean and the Middle East. *J. Geophys. Res. Atmos.*, **117**, https://doi.org/10.1029/2011JD017293.

Tao, L., and Y. Lan, 2017: Inter-decadal change of the inter-annual relationship between the frequency of intense tropical cyclone over the western North Pacific and ENSO. *Int. J. Climatol.*, **37**, 4880–4895, https://doi.org/10.1002/joc.5129.

Taylor, K. E., 2001: Summarizing multiple aspects of model performance in a Single Diagram. *J. Geophys. Res.*, **106**, 7183–7192, https://doi.org/10.1029/2000JD900719.

Taylor, K. E., R. J. Stouffer, and G. A. Meehl, 2012: An Overview of CMIP5 and the experiment design. *Bull. Am. Meteorol. Soc.*, **93**, 485–498,

https://doi.org/10.1175/BAMS-D-11-00094.1.

USDA, 2019: *Grain: World Markets and Trade*. New York, USA: United States Department of Agriculture (USDA). 11 pp. https://www.usda.gov/.

Villarini, G., R. Goska, J. A. Smith, and G. A. Vecchi, 2014: North atlantic tropical cyclones and U.S. flooding. *Bull. Am. Meteorol. Soc.*, **95**, 1381–1388, https://doi.org/10.1175/BAMS-D-13-00060.1.

van Vuuren, D. P., and Coauthors, 2011: The representative concentration pathways: An overview. *Clim. Change*, **109**, 5–31, https://doi.org/10.1007/s10584-011-0148-z.

Walsh, K. J. E., and Coauthors, 2015: Hurricanes and climate, The U.S. CLIVAR Working Group on Hurricanes. *Bull. Am. Meteorol. Soc.*, **96**, 997–1017, https://doi.org/10.1175/BAMS-D-13-00242.1.

Walsh, K. J. E., and Coauthors, 2016: Tropical cyclones and climate change. *Wiley Interdiscip. Rev. Clim. Chang.*, **7**, 65–89, https://doi.org/10.1002/wcc.371.

Wang, A., and X. Zeng, 2012: Evaluation of multireanalysis products with in situ observations over the Tibetan Plateau. *J. Geophys. Res. Atmos.*, **117**, 1–12, https://doi.org/10.1029/2011JD016553.

Wang, B., and J. C. L. Chan, 2002: How strong ENSO events affect tropical storm activity over the western North Pacific. *J. Clim.*, **15**, 1643–1658, https://doi.org/10.1175/1520-0442(2002)015<1643:HSEEAT>2.0.CO;2.

Wang, B., and L. Ho, 2002: Rainy Season of the Asian – Pacific Summer Monsoon. *J. Clim.*, **15**, 386–398.

Wang, L., R. Huang, and R. Wu, 2013: Interdecadal variability in tropical cyclone frequency over the South China Sea and its association with the Indian Ocean sea surface temperature. *Geophys. Res. Lett.*, **40**, 768–771, https://doi.org/10.1002/grl.50171.

Wang, W., H. Lu, D. Yang, K. Sothea, Y. Jiao, B. Gao, X. Peng, and Z. Pang, 2016: Modelling hydrologic processes in the Mekong River basin using a distributed model driven by satellite precipitation and rain gauge observations. *PLoS One*, **11**, 1–19, https://doi.org/10.1371/journal.pone.0152229.

Wang, Y., 2012: Recent Research Progress on Tropical Cyclone Structure and Intensity. *Trop. Cyclone Res. Rev.*, **1**, 254–275, https://doi.org/10.6057/2012TCRR02.05.

Ward, P. J., S. Eisner, M. Flo Rke, M. D. Dettinger, and M. Kummu, 2014: Annual flood sensitivities to el nintild;O-Southern Oscillation at the global scale. *Hydrol. Earth Syst. Sci.*, **18**, 47–66, https://doi.org/10.5194/hess-18-47-2014.

Watanabe, M., and Coauthors, 2010: Improved climate simulation by MIROC5: Mean states, variability, and climate sensitivity. *J. Clim.*, **23**,

6312–6335, https://doi.org/10.1175/2010JCLI3679.1.

Weinkle, J., R. Maue, and R. Pielke, 2012: Historical global tropical cyclone landfalls. *J. Clim.*, **25**, 4729–4735, https://doi.org/10.1175/JCLI-D-11-00719.1.

Winsemius, H. C., and Coauthors, 2016: Global drivers of future river flood risk. *Nat. Clim. Chang.*, **6**, 381–385, https://doi.org/10.1038/nclimate2893.

WMO, 2014: *Atlas of mortality and economic losses from weather, climate and water extremes, 1970 to 2012*. World Meteorological Organization. Geneva, Switzerland.

WMO, 2017: *Global Guide to Tropical Cyclone Forecasting*. World Meteorological Organization. Geneva, Switzerland. 399 pp.

Wong, J. S., S. Razavi, B. R. Bonsal, H. S. Wheater, and Z. E. Asong, 2017: Inter-comparison of daily precipitation products for large-scale hydro-climatic applications over Canada. *Hydrol. Earth Syst. Sci.*, **21**, 2163–2185, https://doi.org/10.5194/hess-21-2163-2017.

Woodruff, J. D., J. L. Irish, and S. J. Camargo, 2013: Coastal flooding by tropical cyclones and sea-level rise. *Nature*, **504**, 44–52, https://doi.org/10.1038/nature12855.

Wu, F., X. Wang, Y. Cai, and C. Li, 2016: Spatiotemporal analysis of precipitation trends under climate change in the upper reach of Mekong River basin. *Quat. Int.*, **392**, 137–146, https://doi.org/10.1016/j.quaint.2013.05.049.

Wu, L., B. Wang, and S. Geng, 2005: Growing typhoon influence on east Asia. *Geophys. Res. Lett.*, **32**, 1–4, https://doi.org/10.1029/2005GL022937.

Yatagai, A., K. Kamiguchi, O. Arakawa, A. Hamada, N. Yasutomi, and A. Kitoh, 2012: Aphrodite constructing a long-term daily gridded precipitation dataset for Asia based on a dense network of rain gauges. *Bull. Am. Meteorol. Soc.*, **93**, 1401–1415, https://doi.org/10.1175/BAMS-D-11-00122.1.

Yeh, S. W., S. K. Kang, B. P. Kirtman, J. H. Kim, M. H. Kwon, and C. H. Kim, 2010: Decadal change in relationship between western North Pacific tropical cyclone frequency and the tropical Pacific SST. *Meteorol. Atmos. Phys.*, **106**, 179–189, https://doi.org/10.1007/s00703-010-0057-0.

Zhang, L., K. B. Karnauskas, J. P. Donnelly, and K. Emanuel, 2017a: Response of the North Pacific tropical cyclone climatology to global warming: Application of dynamical downscaling to CMIP5 models. *J. Clim.*, **30**, 1233–1243, https://doi.org/10.1175/JCLI-D-16-0496.1.

Zhang, Q., X. Gu, P. Shi, and V. P. Singh, 2017b: Impact of tropical cyclones on flood risk in southeastern China: Spatial patterns, causes and

implications. *Glob. Planet. Change*, **150**, 81–93, https://doi.org/10.1016/j.gloplacha.2017.02.004.

Zhang, Q., Y. Lai, X. Gu, P. Shi, and V. P. Singh, 2018: Tropical Cyclonic Rainfall in China: Changing Properties, Seasonality, and Causes. *J. Geophys. Res. Atmos.*, **123**, 4476–4489, https://doi.org/10.1029/2017JD028119.

Zhou, Y., and C. J. Matyas, 2017: Spatial characteristics of storm-total rainfall swaths associated with tropical cyclones over the Eastern United States. *Int. J. Climatol.*, **37**, 557–569, https://doi.org/10.1002/joc.5021.

Zhu, L., S. M. Quiring, and K. A. Emanuel, 2013: Estimating tropical cyclone precipitation risk in Texas. *Geophys. Res. Lett.*, **40**, 6225–6230, https://doi.org/10.1002/2013GL058284